



저작자표시-비영리-변경금지 2.0 대한민국

이용자는 아래의 조건을 따르는 경우에 한하여 자유롭게

- 이 저작물을 복제, 배포, 전송, 전시, 공연 및 방송할 수 있습니다.

다음과 같은 조건을 따라야 합니다:



저작자표시. 귀하는 원저작자를 표시하여야 합니다.



비영리. 귀하는 이 저작물을 영리 목적으로 이용할 수 없습니다.



변경금지. 귀하는 이 저작물을 개작, 변형 또는 가공할 수 없습니다.

- 귀하는, 이 저작물의 재이용이나 배포의 경우, 이 저작물에 적용된 이용허락조건을 명확하게 나타내어야 합니다.
- 저작권자로부터 별도의 허가를 받으면 이러한 조건들은 적용되지 않습니다.

저작권법에 따른 이용자의 권리는 위의 내용에 의하여 영향을 받지 않습니다.

이것은 [이용허락규약\(Legal Code\)](#)을 이해하기 쉽게 요약한 것입니다.

[Disclaimer](#)

A Thesis for the Degree of Master of Science

**Effect of the emulsifier-type on physicochemical properties of
solid lipid nanoparticles applied as food-Pickering stabilizers**

식품 피커링 안정제로 활용되는 고형지질나노입자의
물리화학적 특성에 미치는 유화제 유형의 영향

February, 2019

Honggu Lim

Department of Agricultural Biotechnology

Seoul National University

농학석사학위논문

**Effect of the emulsifier-type on physicochemical properties of
solid lipid nanoparticles applied as food-Pickering stabilizers**

식품 피커링 안정제로 활용되는 고형지질나노입자의
물리화학적 특성에 미치는 유화제유형의 영향

지도교수 최영진

이 논문을 석사학위 논문으로 제출함

2019년 2월

서울대학교 대학원 농생명공학부

임 홍 구

임홍구의 석사 학위 논문을 인준함

2019년 2월

위원장 서진호 (인)

부위원장 최영진 (인)

위원 유상열 (인)

ABSTRACT

Many studies using solid lipid nanoparticles (SLNs) as a Pickering stabilizer have been conducted. SLNs have the advantage of food-grade, inexpensive, ease of preparation and easy for adjusting the characteristics. As a Pickering stabilizer, SLNs can be applied to both oil-in-water and water-in-oil system depending on characteristics such as wettability. SLNs-stabilized Pickering emulsion has enhanced physical stability than conventional emulsifier-stabilized emulsion. In this study, I verified effects of type/concentration of the emulsifiers (Tween 60, Brij S20, and Brij S100) on physicochemical characteristics of SLNs and investigated the properties of the emulsion stabilized by the SLNs. With increase of the emulsifier-concentration, surface load and α -form crystal increased while the β' / β -form crystals tended to decrease. In order to minimize the stabilizing effect of free emulsifier, the remaining emulsifier was removed via dialysis and the contact angle was measured. The contact angle of SLNs tended to decrease as the surface load of the emulsifier and the formation of α -form crystal increased and β' / β -form crystal decreased. The contact angles of SLNs stabilized with Tween 60, Brij S20 and Brij S100 at the saturation concentration of emulsifier were about 140, 135 and 150 °, respectively. The contact angle of SLNs seem

to be more influenced by the type of lipid crystal formed than the surface load of emulsifier. The stability of SLNs-stabilized oil-in-water Pickering emulsion was also evaluated. Under the experimental conditions, the stability of Pickering emulsion showed a tendency to become higher as the contact angle of SLNs and the negative value of ζ -potential decreased. When SLNs made with saturated concentration of each emulsifier were used as a Pickering stabilizer, it maintained a constant size distribution for more than 4 weeks. Our results can be versatily applied in utilizing Pickering emulsion using SLNs and will create a new viewpoint in the production of new delivery system.

Keywords: Pickering emulsion, solid lipid nanoparticles, SLNs, emulsifier, wettability, contact angle, surface load

Student Number: 2017-25766

CONTENTS

ABSTRACT	II
CONTENTS	IV
LIST OF FIGURES	VI
LIST OF TABLES	XI
I. INTRODUCTION	1
II. MATERIALS AND METHODS	5
2.1. Materials.....	5
2.2. Preparation of solid lipid nanoparticles (SLNs).....	5
2.3. Preparation of oil-in-water emulsions.....	8
2.4. Measurement of size and ζ -potential of SLNs.....	10
2.5. Measurement of size of emulsions.....	10
2.6. Polarized microscopic observation.....	11
2.7. Quantification of free emulsifiers.....	11

2.8. Dialysis of SLNs dispersions.....	12
2.9. Differential scanning calorimetry (DSC) measurements.....	13
2.10. Transmission electron microscopy (TEM).....	13
2.11. Measuring the contact angle of SLNs at the oil-water interface.....	14
III. RESULTS AND DISCUSSION.....	17
3.1. Characteristics of the solid lipid nanoparticles.....	17
3.2. Preparation and characteristics of the SLNs-stabilized emulsions.....	48
IV. CONCLUSIONS.....	63
V. REFERENCES.....	65
XI. 국문초록.....	70

LIST OF FIGURES

Figure 1. A schematic representation of the production process of solid lipid nanoparticles (SLNs) dispersions.....	7
Figure 2. A schematic representation of the production process of emulsions stabilized with solid lipid nanoparticles (SLNs).....	9
Figure 3. A schematic representation of the gel-trapping technique and the visualization of micromorphology of the trapped particles using atomic force microscopy.....	16
Figure 4. Z-average and PDI value of Tween 60-stabilized solid lipid nanoparticles.....	19
Figure 5. Z-average and PDI value of Brij S20-stabilized solid lipid nanoparticles.....	20
Figure 6. Z-average and PDI value of Brij S100-stabilized solid lipid nanoparticles.....	21
Figure 7. D_{3,2} value of Tween 60, Brij S20, Brij S100-stabilized solid lipid nanoparticles (SLNs).....	22

Figure 8. Values for ζ-potential of Tween 60-, Brij S20-, Brij S100-stabilized solid lipid nanoparticles (SLNs).....	23
Figure 9. Values for z-average and ζ-potential of Tween 60-stabilized solid lipid nanoparticles at pH 3-7 (25 °C).....	25
Figure 10. Values for z-average and ζ-potential of Brij S20-stabilized solid lipid nanoparticles at pH 3-7 (25 °C).....	26
Figure 11. Values for z-average and ζ-potential of Brij S100-stabilized solid lipid nanoparticles at pH 3-7 (25 °C).....	27
Figure 12. Melting and crystallization thermograms of bulk tristearin in the differential scanning calorimetry.....	31
Figure 13. Melting thermograms of Tween 60-stabilized solid lipid nanoparticles in the differential scanning calorimetry.....	32
Figure 14. Melting thermograms of Brij S20-stabilized solid lipid nanoparticles in the differential scanning calorimetry.....	33
Figure 15. Melting thermograms of Brij S100-stabilized solid lipid nanoparticles in the differential scanning calorimetry.....	34
Figure 16. Transmission electron micrographs of the solid lipid nanoparticles stabilized with 10 mmol/kg of Tween 60.....	36

Figure 17. Transmission electron micrographs of the solid lipid nanoparticles stabilized with 10 mmol/kg of Brij S20.....	37
Figure 18. Transmission electron micrographs of the solid lipid nanoparticles stabilized with 3 mmol/kg of Brij S100.....	38
Figure 19. Atomic force micrograph of the polydimethylsiloxane-embedded solid lipid nanoparticles stabilized with 10 mmol/kg of Tween 60.....	40
Figure 20. Atomic force micrograph of the polydimethylsiloxane-embedded solid lipid nanoparticles stabilized with 10 mmol/kg of Brij S20.....	41
Figure 21. Atomic force micrograph of the polydimethylsiloxane-embedded solid lipid nanoparticles stabilized with 3 mmol/kg of Brij S100.....	42
Figure 22. A schematic representation of calculating contact angle of solid lipid nanoparticles embedded at the interface.....	43
Figure 23. Contact angle of Tween 60-stabilized solid lipid nanoparticles (SLNs) in the oil-water interface, and surface load of the SLNs.....	45

Figure 24. Contact angle of Brij S20-stabilized solid lipid nanoparticles (SLNs) in the oil-water interface, and surface load of the SLNs.....46

Figure 25. Contact angle of Brij S100-stabilized solid lipid nanoparticles (SLNs) in the oil-water interface, and surface load of the SLNs.....47

Figure 26. Polarized light micrograph of the hand-shaking emulsions prepared with 1 wt% of the Tween 60 (24 mmol/kg)-stabilized solid lipid nanoparticles and 10 wt% of canola oil.....52

Figure 27. Polarized light micrograph of the hand-shaking emulsions prepared with 1 wt% of the Brij S20 (24 mmol/kg)-stabilized solid lipid nanoparticles and 10 wt% of canola oil.....53

Figure 28. Polarized light micrograph of the hand-shaking emulsions prepared with 1 wt% of the Brij S100 (8 mmol/kg)-stabilized solid lipid nanoparticles and 10 wt% of canola oil.....54

Figure 29. Particle size distribution of the emulsions prepared with 1 wt% of the Tween 60 (10 and 24 mmol/kg)-stabilized solid lipid nanoparticles and 10 wt% canola oil after 0, 10, 20 and 31 day-storage.....56

Figure 30. Particle size distribution of the emulsions prepared with 1 wt% of the Brij S20 (10 and 24 mmol/kg)-stabilized solid lipid nanoparticles and 10 wt% canola oil after 0, 10, 20 and 31 day-storage.....59

Figure 31. Particle size distribution of the emulsions prepared with 1 wt% of the Brij S100 (3 and 8 mmol/kg)-stabilized solid lipid nanoparticles and 10 wt% canola oil after 0, 10, 20 and 31 day-storage.....62

LIST OF TABLES

Table 1. The amount of the Pickering emulsion-covering emulsifiers bound and unbound on the surface of the solid lipid nanoparticles (SLNs)	
.....	50

I. INTRODUCTION

Emulsions generally mean a system stabilized by mixing two immiscible liquids, such as oil and water. These lipid carrier systems can encapsulate bioactive materials and increase bioavailability. Thereby, emulsions are being applied in various aspects such as cosmetics, pharmaceuticals and foods from an industrial point of view. In conventional production of emulsions, small amphipathic molecules usually used as emulsifiers, such as phospholipids, proteins, etc. which is attached to the oil-water interface during the emulsification process and forms a barrier at the interface to protect the emulsion droplet from aggregation or coalescence (McClements, 2015).

However, emulsions stabilized with these conventional emulsifiers are vulnerable to phenomena such as coalescence. Particle-stabilized emulsions have been studied to improve these disadvantages and increase emulsion stability (Pickering, 1907).

Physicochemical aging of emulsion is closely related to the structure and composition of the interfacial layer (Berton-Carabin & Schroën, 2015). Particle-stabilized emulsion is strong against coalescence (Dickinson, 2010;

Pichot, Spyropoulos, & Norton, 2009), lipid oxidation (Monteillet et al., 2014; Schröder, Corstens, Ho, Schroën, & Berton-Carabin, 2018), shear (Kotula & Anna, 2012; Thompson, Williams, & Armes, 2015). Studies are also being conducted to partially or fully replace the emulsifier with natural ingredients in the food industry and studies on this direction have been actively conducted (French et al., 2016; Morris, 2011). Various food-grade particles such as OSA-modified starch (Timgren, Rayner, Sjöo, & Dejmeck, 2011), wax crystal (Binks & Rocher, 2009) and CaCO₃ (Zhou, Cao, Liu, & Stoyanov, 2009) among various organic and inorganic origin particles are being studied.

The stability and effectiveness of these various Pickering stabilizers are strongly influenced by wettability, shape, and size (Leal-Calderon & Schmitt, 2008). For example, if the Pickering stabilizer is hydrophilic, it is more wetted to water and oil-in-water system is preferred. If the Pickering stabilizer is hydrophobic, the particles are more wetted to the oil and the water-in-oil system is preferred (Aveyard, Binks, & Clint, 2003; Dickinson, 2010; Finkle, Draper, & Hildebrand, 1923).

Pickering stabilizers are strongly attached to the oil-water interface and the bond energy can be expressed as ΔG_a :

$$\Delta G_a = \pi r^2 \gamma_{ow} (1 - \cos \theta)^2$$

Where r is the diameter of the particle, γ is the interfacial tension between the two immiscible liquids, and θ is the contact angle. Even in small particles, the bond energy is very strong, making irreversible adhesion and acting as a stable stabilizer (Schröder et al., 2017).

Lately, various studies using fat crystals have been conducted (Gupta & Rousseau, 2012; Pawlik, Kurukji, Norton, & Spyropoulos, 2016; Schröder, Sprakel, Schroën, & Berton-Carabin, 2017; I Zafeiri, Smith, Norton, & Spyropoulos, 2017). Lipid-based particles such as fat crystals are known to be effective stabilizers for stabilizing water-in-oil emulsions such as spreads (Dickinson, 2012; Frasc-Melnik, Norton, & Spyropoulos, 2010; Rousseau, 2000, 2013). However, studies on the properties of solid lipid nanoparticles (SLNs) such as contact angle and stabilization effect attributed by the type and concentration of emulsifier are insufficient. Therefore, in this study, I studied the effect of the type and concentration of the emulsifier used to impart hydrophilicity to SLNs. In addition, I tried to utilize SLNs for oil-in-water emulsion which can be highly utilized in various fields.

PEGylated emulsifiers were used in this study for the construction of model system because it is safe for human body (Nagaoka & Nakao, 1990). It is widely used in various fields such as cosmetics, pharmaceuticals, foods and

easy to adjust PEG chain length. Tween 60 and Brij S20 were used in this experiment to observe differences mediated by molecular structures between emulsifiers with similar HLB values and molecular weights. Brij S20 and Brij S100 were used to observe the effect of emulsifier's hydrophilicity mediated by PEG chain length although they have the same structure. In addition, dialysis of SLNs were conducted to confirm that stabilization by SLNs solely was possible by excluding the influence of free emulsifier.

Based on the results of the previous study (Ban, Jo, Lim, & Choi, 2018), it is also thought that the absorption pattern of emulsion in the human body can be controlled by manufacturing the characteristics of the SLNs using the PEGylated emulsifier. And two lipophilic substances can be loaded into the particle and emulsion droplet, respectively, so that absorption in the body with time difference controlled release can be possible.

II. MATERIAL AND METHODS

2.1. Materials

Tristearin (Dynasan 118) was kindly provided from IOI Oleo (IOI Oleochemicals GmbH, Germany). Polyoxyethylene (20) sorbitanmonostearate (Tween 60, HLB = 14.9), Polyoxyethylene (20) stearylether (Brij S20, HLB = 15.0) and Polyoxyethylene (100) stearylether (Brij S100, HLB = 18.0) were purchased from Sigma Aldrich (UK). Vivaspin 6 (PES, 1000 kDa) was purchased from Sartorius (UK). Dialysis tubing (Biotech CE Membrane, 1000 kDa) was purchased from Spectrum lab (USA). Canola oil was purchased from the local supermarket. All materials were used without further purification or modification.

2.2. Preparation of solid lipid nanoparticles (SLNs)

Tristearin of 2.5 wt% was added to the 0.02 wt% sodium azide solution containing 10, 13, 16, 20 and 24 mmol/kg of emulsifier (Tween 60, Brij S20) or 3, 4.5, 6, 8 and 10 mmol/kg of emulsifier (Brij S100). The total weight was adjusted to 100 g. After that, heating was carried out at 80 °C water

bath for 60 minutes. Then, premix was processed with ultrasound in 80 °C jacket beaker using a sonicating probe (VCX 750, Sonics & Materials Inc., USA) for 7 min at 60 % amplitude, a duty cycle of 1 s (Fig 1). The dispersion was cooled down in the ice bath for overnight and then stored in a refrigerator at 4 °C.

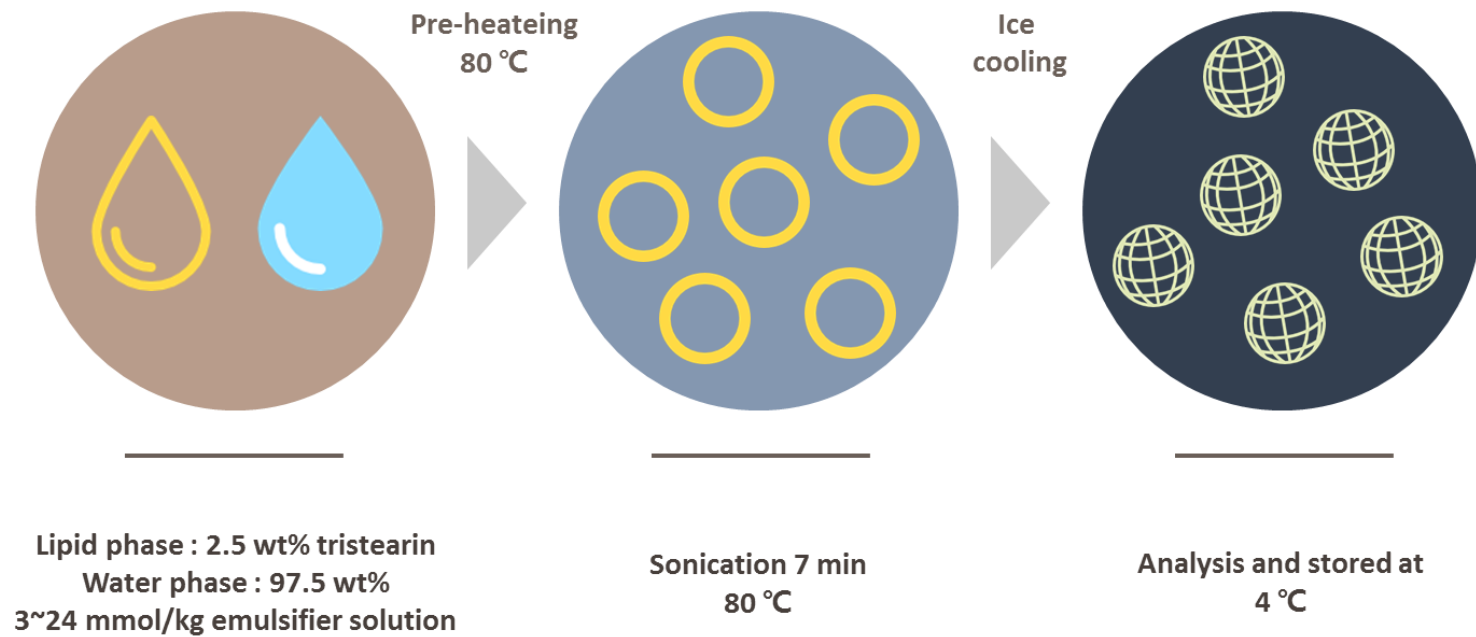


Figure 1. A schematic representation of the production process of solid lipid nanoparticles (SLNs) dispersions.

2.3. Preparation of oil-in-water emulsions

The oil-in-water emulsion was prepared by adding 8.3 g of canola oil to 75 g of 1 wt% SLNs dispersion. Premix were then homogenized with a high-speed blender (Ultra-Turrax T25D, Ika werke GmbH & Co., Germany) at 7,000 rpm for 2 min. After preparing the coarse emulsion, the droplet size was further reduced by sonication (VCX 750, Sonics & Materials Inc., USA) for 1 min at 60 % amplitude, a cycles of 1 s on / 3 s off. To prevent shear or heat-induced melting of SLNs, the mixture was processed in a 2 °C jacket beaker during emulsification (Fig 2). The prepared emulsion was analyzed immediately and after 10, 20 and 31 days storage. All prepared emulsions were stored in a refrigerator at 4 °C.

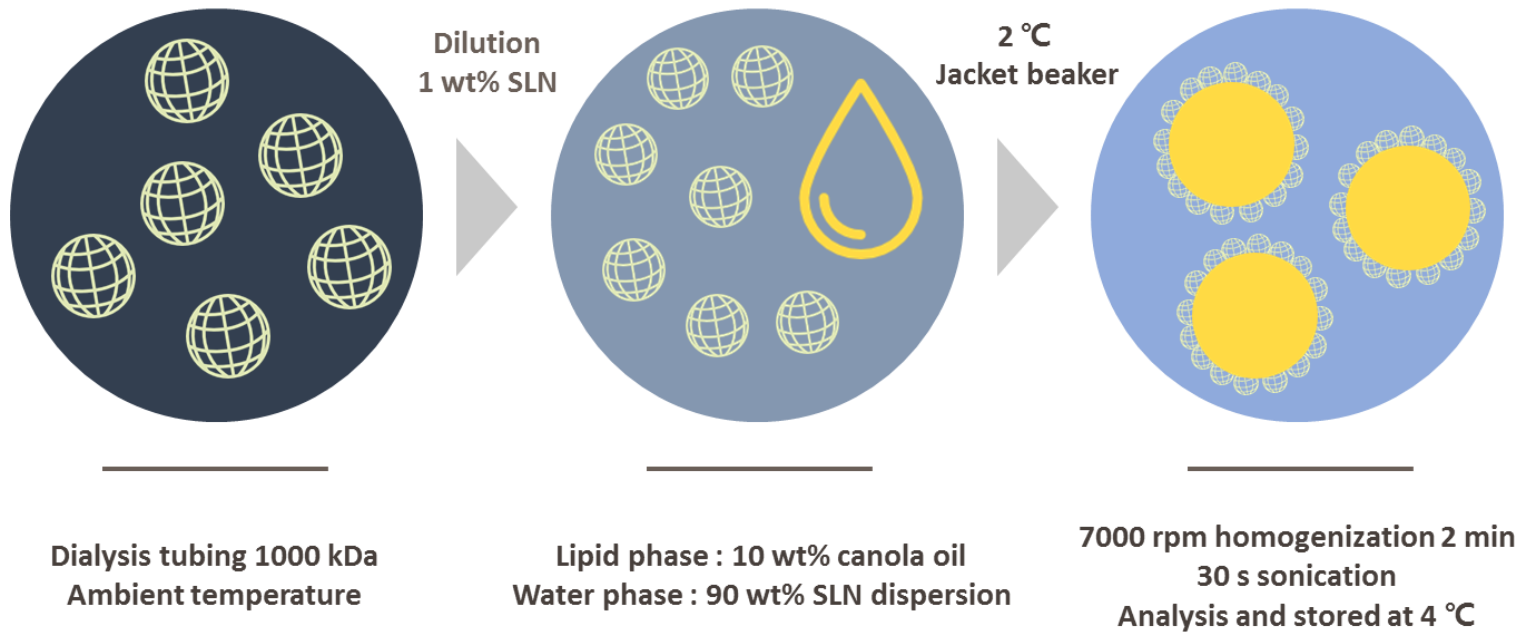


Figure 2. A schematic representation of the production process of emulsions stabilized with solid lipid nanoparticles (SLNs).

2.4. Measurement of size and ζ -potential of SLNs

The prepared SLNs dispersion was treated overnight in ice bath. The dispersion was then diluted 1/200 with distilled water. The size and ζ -potential of SLNs were measured using a Zetasizer (Nano ZS90, Malvern Instruments Ltd., UK). $D_{3,2}$ was also measured using a Malvern Mastersizer 2000S (Malvern Instruments, UK) equipped with a Hydro S dispersion cell. Refractive index of 1.49 (RI of the tristearin) was used to calculate Sauter mean diameter ($D_{3,2}$).

2.5. Measurement of size of emulsions

The droplet size of oil-in-water emulsion was measured to evaluate the stability over time for coalescence. The droplet size distribution was determined by laser diffraction using a Malvern Mastersizer 2000S (Malvern Instruments, UK) equipped with a Hydro S dispersion cell. Refractive index of 1.472 (RI of the canola oil) was used to analyze droplet size distribution. Samples were measured immediately after preparation, 10, 20 and 31 days following emulsion preparation.

2.6. Polarized microscopic observation

Polarized microscopy was used to observe the SLNs stabilized emulsion (Eclipse LV 100 ND, Nikon, Japan). The emulsion for observation was prepared by hand shaking with reference to the method in the previous study (Schröder et al., 2017) for 10 seconds with 4.5 g of 1 wt% SLNs dispersion and 0.5 g of canola oil in a 15 ml tube. The prepared emulsion was diluted to 1/10 and observed.

2.7. Quantification of free emulsifiers

Experiments were conducted to measure the free emulsifier remaining in the dispersion without stabilizing the SLNs. Tween 60, Brij S20, and Brij S100-stabilized SLNs dispersions were diluted 1/20, 1/20, 1/500 with distilled water to determine the free emulsifier remaining in the solution without attaching to the interface of the SLNs. The measurement was carried out before and after dialysis of each of the dispersions. The diluted dispersions were filtered using a syringe filter (Whatman, GD / X PVDF filter, 0.45 μm , 25 mm diameter, Germany) to remove large particles and aggregates. The filtered dispersions were then placed in an ultra-filtration tube (Vivaspin 6,

1000 kDa, Sartorius, UK) to remove SLNs from the dispersion and treated at 2370 RCF, 40 min, 20 °C (Universal 320R centrifuge, Hettich, Germany). After that, 2 ml of filtrate was transferred to a 2 ml tube and dried in an oven at 65 °C for 48 h. The sample was then cooled in ambient conditions and added with 0.5 ml of ammonium cobalthiocyanate (ACTC) solution and 1.0 ml of dichloromethane. The ACTC solution was prepared by adding 3 g of cobalt nitrate hexahydrate and 18 g of ammonium thiocyanate in 100 ml of distilled water. Samples were vortexed for 10 s and then centrifuged at 10,400 g for 10 min (5427R, Eppendorf AG, Hamburg, Germany). After centrifugation, the dichloromethane layer was transferred to a micro quartz cell and absorbance at 625 nm was measured using a spectrophotometer (Pharmaspec UV-1700, Shimadzu Corp., Japan). The amount of emulsifier in the sample was calculated from the standard curves over the ranges of 0.05-1.0, 0.05-1.0 and 0.001-0.01 mmol/kg for Tween 60, Brij S20, and Brij S100 ($R^2 = 0.9996$, 0.9997, 0.9964), respectively.

2.8. Dialysis of SLN dispersions

The emulsifier remaining in the SLNs solution was removed by dialysis to minimize the oil-water interface stabilized by the emulsifier. 30 g

of 2.5 wt% SLNs solution was added to the dialysis tubing (Biotech CE Tubing, 1000 kDa, 131492, Spectrum lab, USA) and dialyzed in a 5 L beaker. SLNs stabilized with Tween 60 or Brij S20 was dialyzed for 1 week and SLNs stabilized with Brij S100 was dialyzed for 3 weeks at ambient temperature. After dialysis, distilled water was added to the SLNs dispersion to make a total weight of 75 g.

2.9. Differential scanning calorimetry (DSC) measurements

Melting and crystallization behaviors of SLNs were measured using a differential scanning calorimeter (Discovery DSC, TA Instruments, Zellik, Belgium). Approximately 5 mg of SLNs dispersion was placed in a hermetic aluminum pan and sealed. An empty pan is used as a reference. Each pan was heated from 25 °C to 95 °C at 3 °C/min and cooled to 10 °C at 3 °C/min. The thermograms are determined using TRIOS software.

2.10. Transmission electron microscopy (TEM)

Transmission electron microscopy (TEM) was used to observe the nanostructure of SLNs. First, SLNs samples were diluted to 0.1 wt% using distilled water and 10 µL were loaded on a film-coated copper grid. After 30

s, the sample was absorbed by filter paper, washed with 10 μL of distilled water. After drying for 30 min, 10 μL of 1 w/v% aqueous solution of phosphotungstic acid was added and negatively stained for 10 min. The overflow phosphotungstic acid solution was wiped off by filter paper and dried on a desiccator for 12 h. Images are recorded on a energy-filtering transmission electron microscope operating at 120 kV (LIBRA 120, Carl Zeiss, Germany).

2.11. Measuring the contact angle of SLNs at the oil-water interface

The contact angle of the SLNs at the oil-water interface was measured by modifying the gel trapping technique (Paunov, 2003). Canola oil was used as oil phase and 1.5 w/v% gellan was added to 0.5 mM CaCl_2 solution as a water phase. PDMS and Sygard 184 elastomer were used as curing agent in a ratio of 10:1. First, dissolve the gellan solution by autoclaving at 121 $^\circ\text{C}$ for 15 minutes, and transfer 20 ml of the solution to the cell culture dish. Then pour 20 ml of canola oil onto the gellan solution and shake it gently to create a flat oil-water interface. In order to carry out the experiment at a temperature lower than the melting point of SLNs, the cell culture dishes are equilibrated by incubating in a 42 $^\circ\text{C}$ incubator for 1 h. 0.3 ml of dialyzed 0.5 wt% SLNs

solution are injected into the oil-water surface. The cell culture dish was shaken sufficiently to place the SLNs on the oil-water interface as a monolayer. Solidification of aqueous gel was performed at ambient temperature. The oil phase was removed and PDMS was added. Solidification of PDMS was performed at ambient temperature for 48 h. The layer of PDMS was peeled off from aqueous gel and washed with distilled water.

Surficial morphology of the layer of PDMS was analyzed by atomic force microscopy (Cypher S Atomic Force Microscope, Asylum Research, Santa Barbara, CA, USA) to measure the contact angle of SLNs at the oil-water interface. The observation was performed using a standard non-contact probe (PR-T300, Probes, Seongnam, Korea) in AC mode (Fig 3).

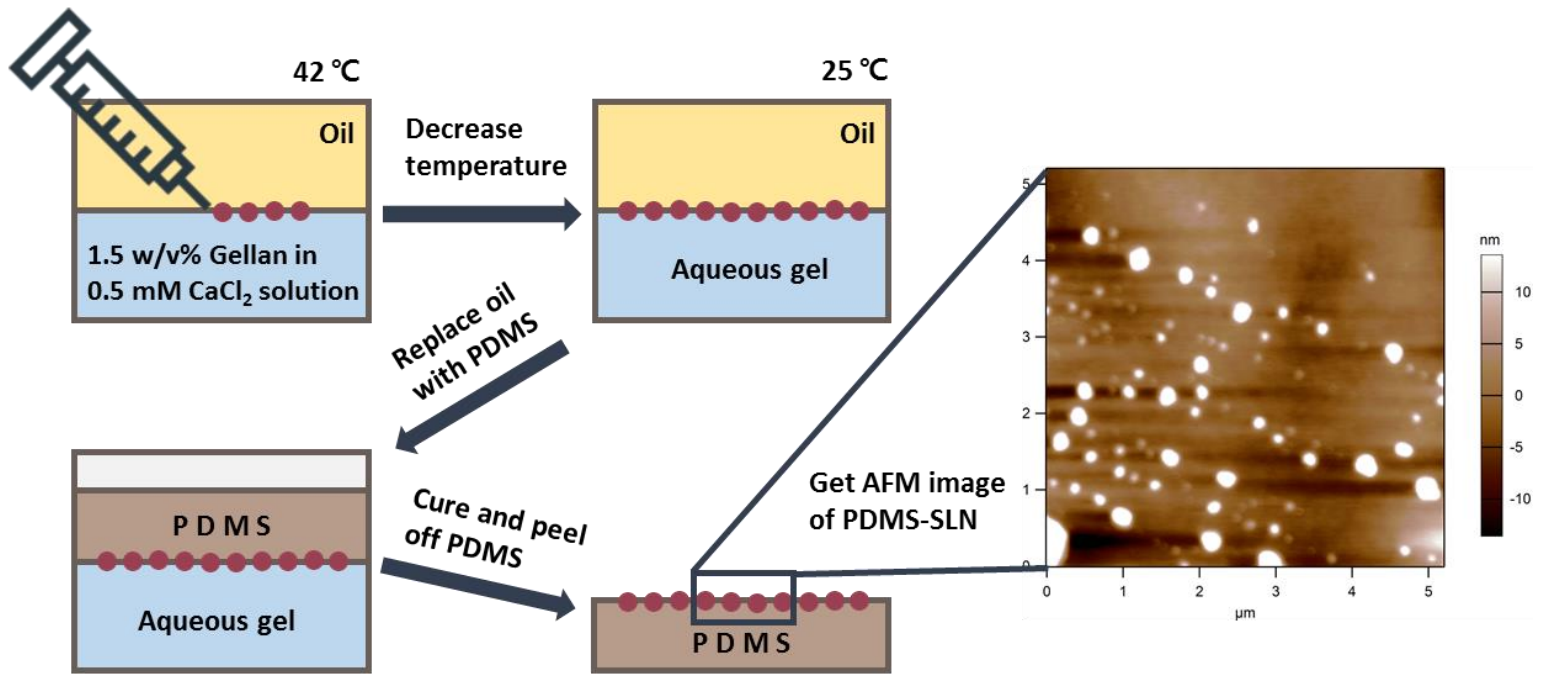


Figure 3. A schematic representation of the gel-trapping technique and the visualization of micromorphology of the trapped particles using atomic force microscopy.

III. RESULTS AND DISCUSSION

3.1. Characteristics of the solid lipid nanoparticles

After incubation with tristearin in emulsifier solution, SLNs were prepared at 80 °C by hot sonication method. Z-average and ζ -potential were measured by dynamic light scattering and $D_{3,2}$ was measured by static light scattering.

The minimum emulsifier concentration was set as a concentration at which the size distribution of SLNs was unimodal and not gelled during dialysis. The maximum emulsifier concentration was set to the region where the formed SLNs sizes were increased or bimodally formed. Tween 60 and Brij S20 were used at concentrations of 10, 13, 16, 20 and 24 mmol / kg, and Brij S100 at concentrations of 3, 4.5, 6, 8 and 10 mmol / kg.

Z-average and $D_{3,2}$ values were about or below 200 nm after dialysis in most experimental concentrations (Fig 4, 5, 6, 7). After dialysis, the z-average tended to increase slightly. $D_{3,2}$ value was used to measure the surface load, and z-average value was used to measure the contact angle. The ζ -potential value of the Brij S20-stabilized SLNs is about -5 mV, which is close

to 0 mV. Tween 60 or Brij S100-stabilized SLNs showed the ζ -potential value of about -20 mV (Fig 8). Tween 60 and Brij S20 have almost the same molecular weight and HLB value, but SLNs stabilized with both emulsifiers have a large difference in zeta-potential value. It is considered that this is due to the difference in the surface load or adhesion state due to the structural difference of the two emulsifiers.

Tween 60 is a form of PEG chain randomly bound to sorbitan. Brij S20 is a form in which stearic acid and PEG chains are bonded to an ether bond. Due to this difference, Tween 60 can be expressed in the form of an inverted triangle and Brij S20 can be expressed in the form of a line. Therefore, Tween 60 occupies a larger volume of space than Brij S20, and therefore surface load at SLNs is also lower. This suggests that the tween 60-stabilized SLNs are exposed to the surface of tristearin relatively more and have a higher negative charge. Likewise, Brij S100 has a longer length of PEG chain than Brij S20, which occupies a large volume spatially, thus saturates at a much lower surface load, so the large portion of the tristearin surface is exposed to the outside, resulting in a low negative charge.

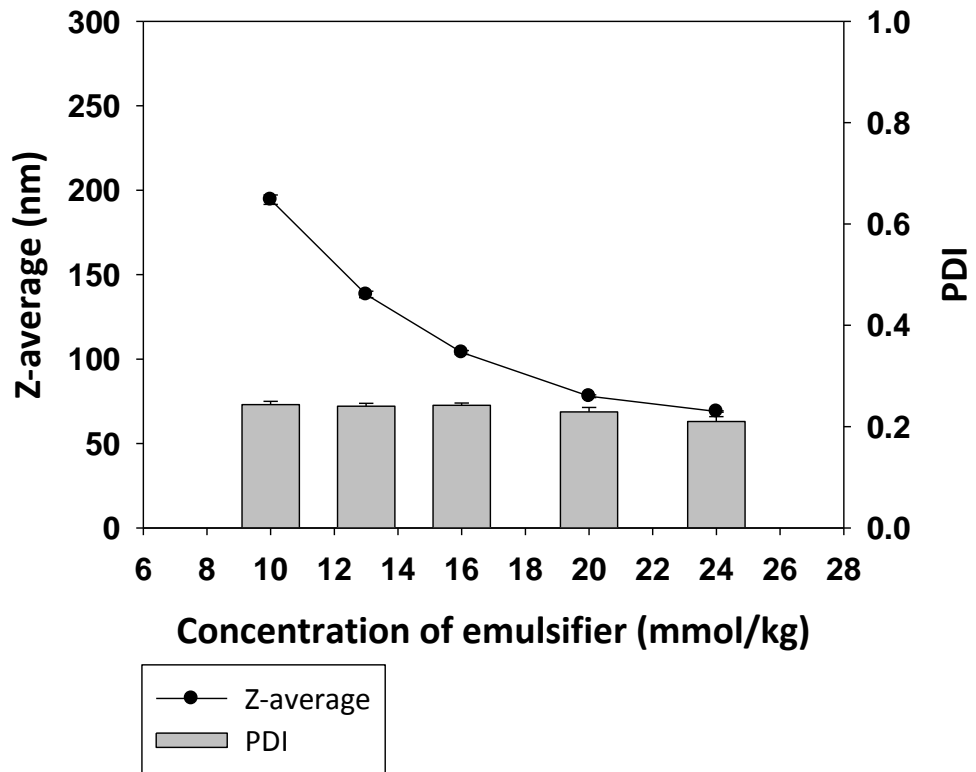


Figure 4. Z-average and PDI value of Tween 60-stabilized solid lipid nanoparticles.

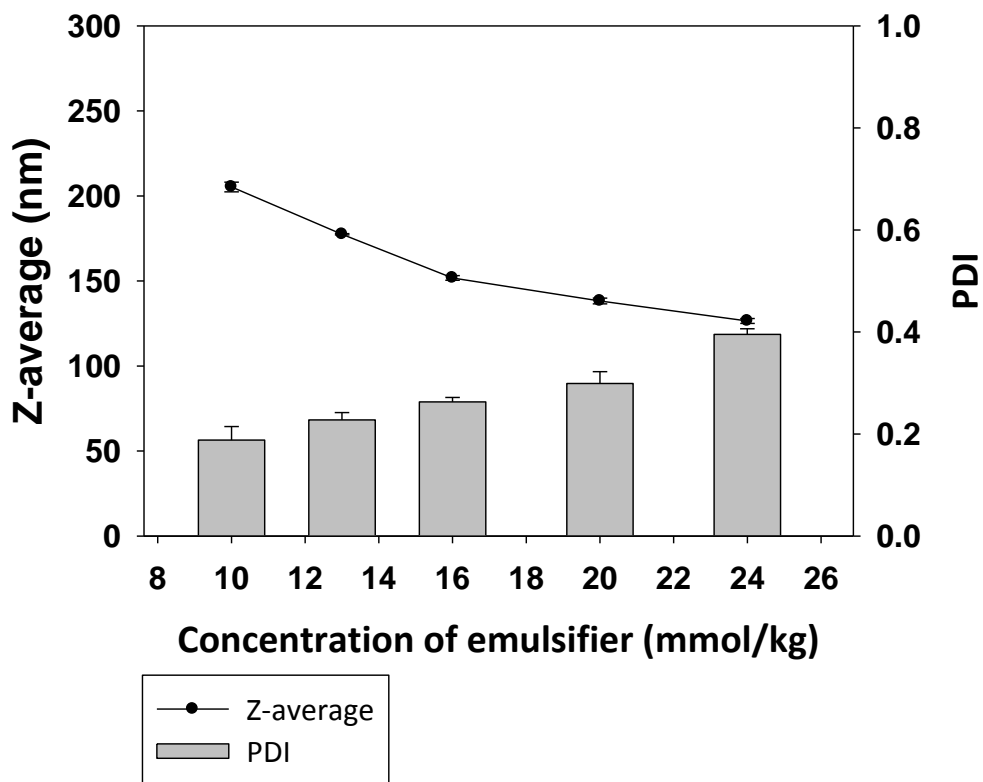


Figure 5. Z-average and PDI value of Brij S20-stabilized solid lipid nanoparticles.

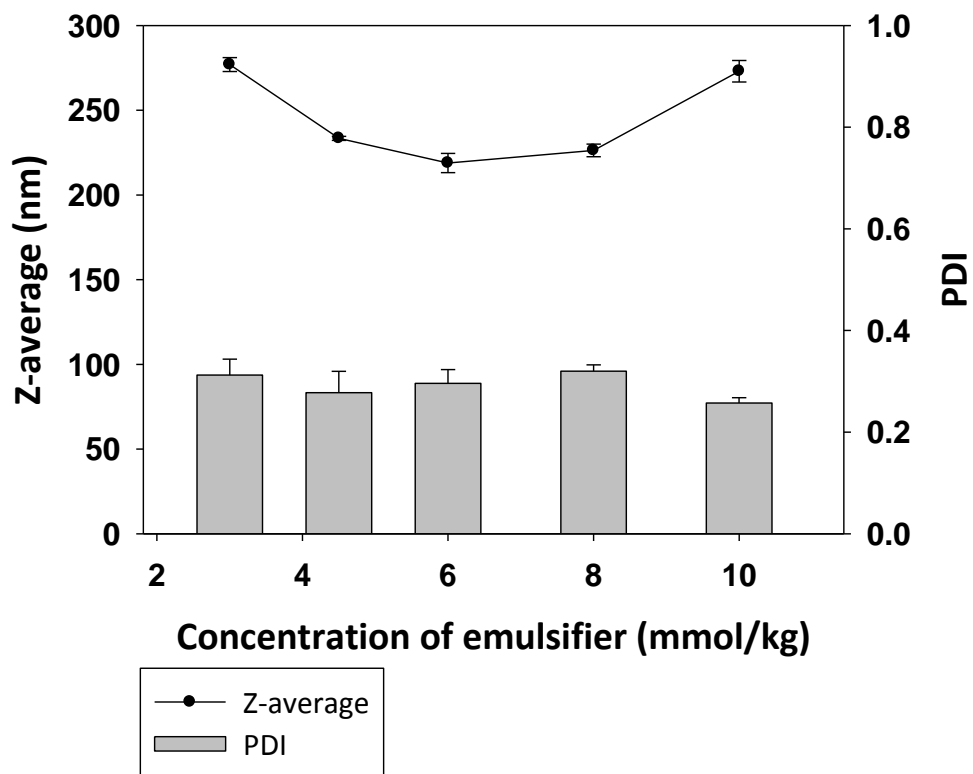


Figure 6. Z-average and PDI value of Brij S100-stabilized solid lipid nanoparticles.

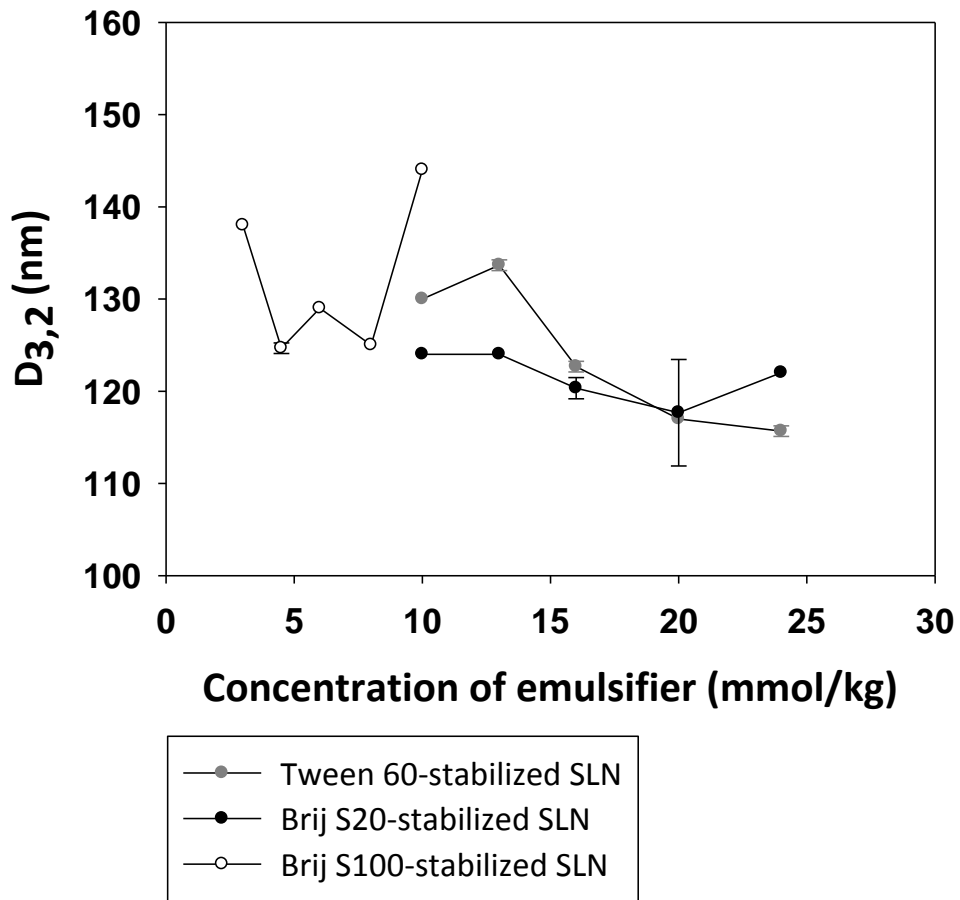


Figure 7. Values for $D_{3,2}$ of Tween 60-, Brij S20-, and Brij S100-stabilized solid lipid nanoparticles (SLNs).

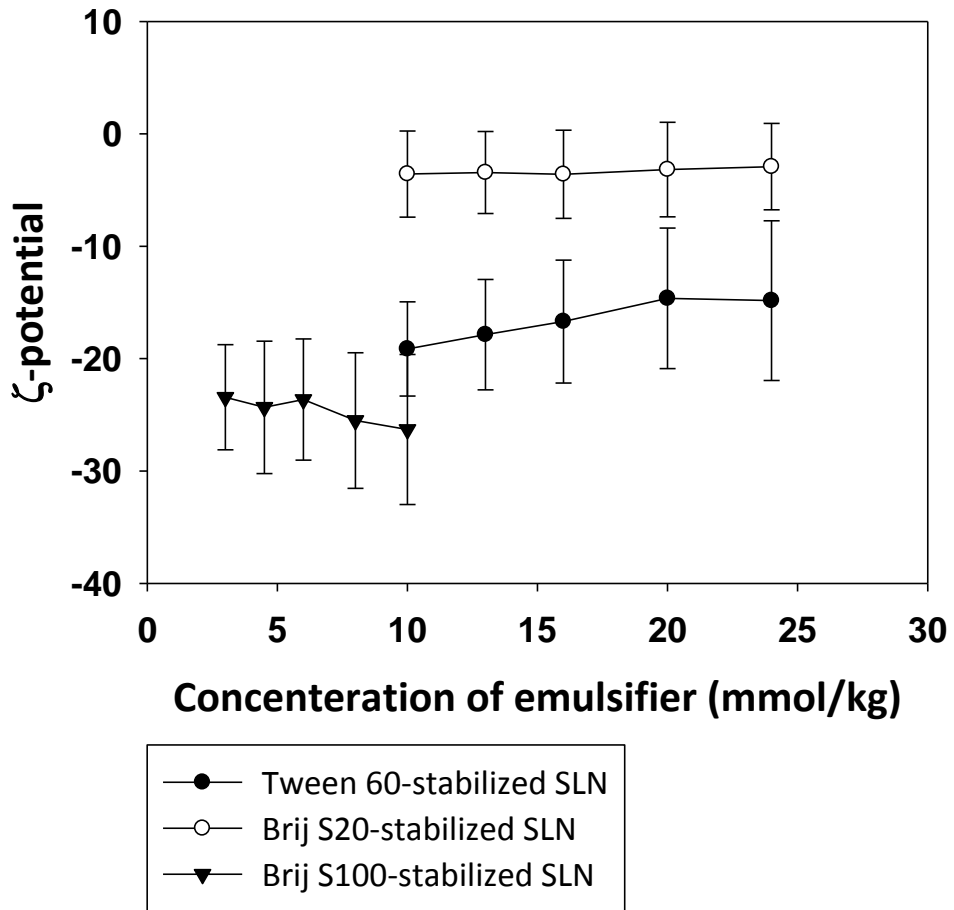


Figure 8. Values for ζ -potential of Tween 60-, Brij S20-, Brij S100-stabilized solid lipid nanoparticles (SLNs).

In order to apply SLNs-stabilized Pickering emulsion to a real food system, SLNs should exhibit stable properties for various environments. Therefore, it is important to understand the stability of the SLNs in a variety of environments, such a pH condition. The pH of the SLNs dispersions were 6-7, and in this experiment, the stability and ζ -potential of SLNs were measured according to pH range 3-7 (Fig 9, 10, 11). Experiments were carried out using the SLNs made up of the minimum and maximum concentrations of emulsifier used in the experiment.

The SLNs stabilized with each emulsifier showed high stability at pH 3-7, and no change in size distribution was observed in both low and high concentrations of emulsifier used in the experiment. The ζ -potential value tended to approach zero as the dispersion acidity increased which was due to the neutralization of the negative charge of the SLNs. The stability of these SLNs will provide excellent steric hindrance for oil droplets when used as Pickering stabilizers. In addition, even if the ζ -potential value of SLNs changes according to the pH change, it is considered that stability of Pickering emulsion is assigned due to negative charge of oil droplet.

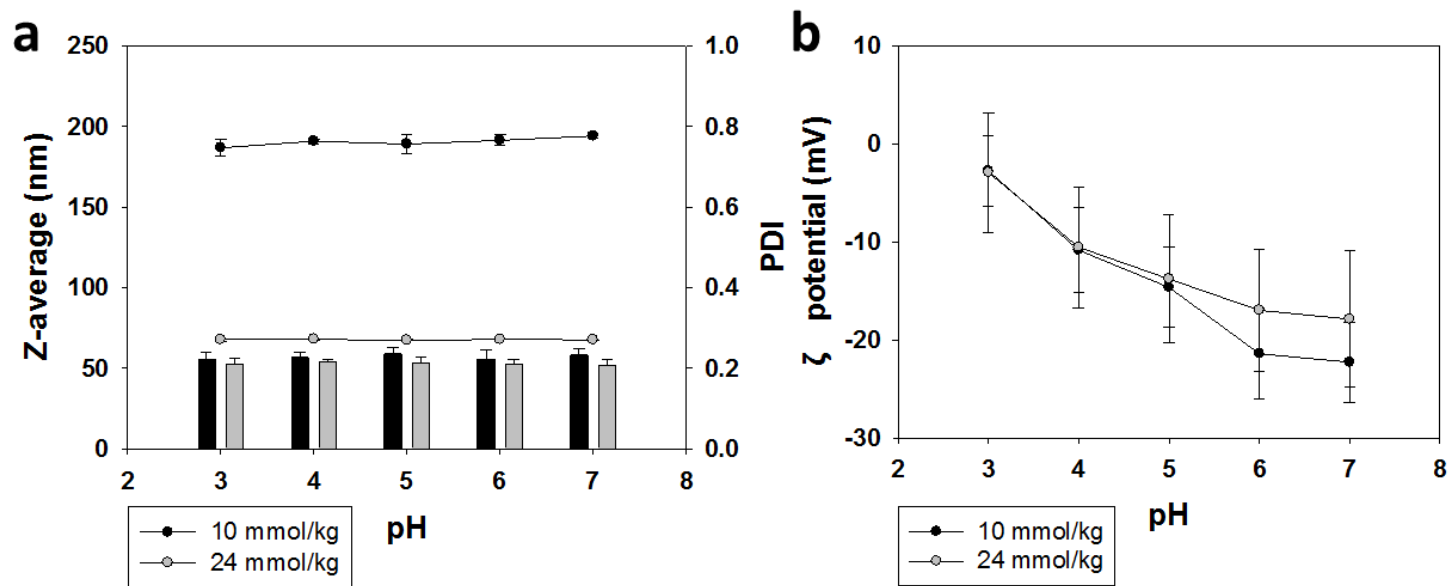


Figure 9. Values for (a) z-average and (b) ζ -potential of Tween 60-stabilized solid lipid nanoparticles at pH 3-7 (25 °C).

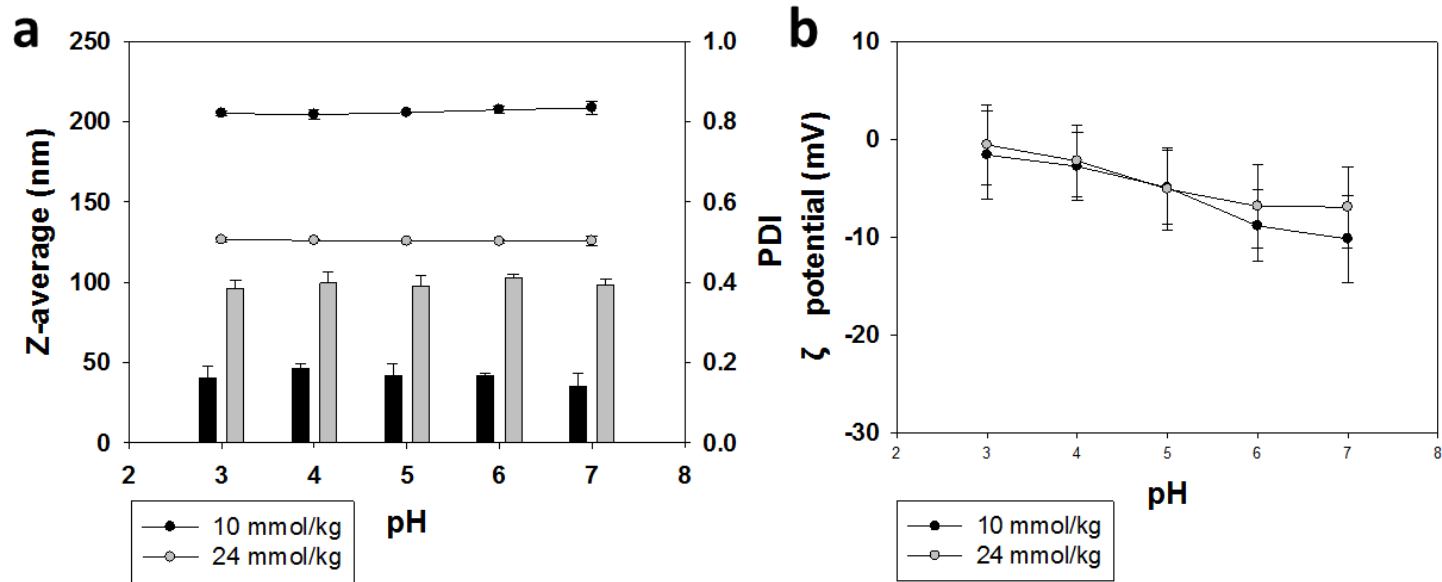


Figure 10. Values for (a) z-average and (b) ζ -potential of Brij S20-stabilized solid lipid nanoparticles at pH 3-7 (25 °C).

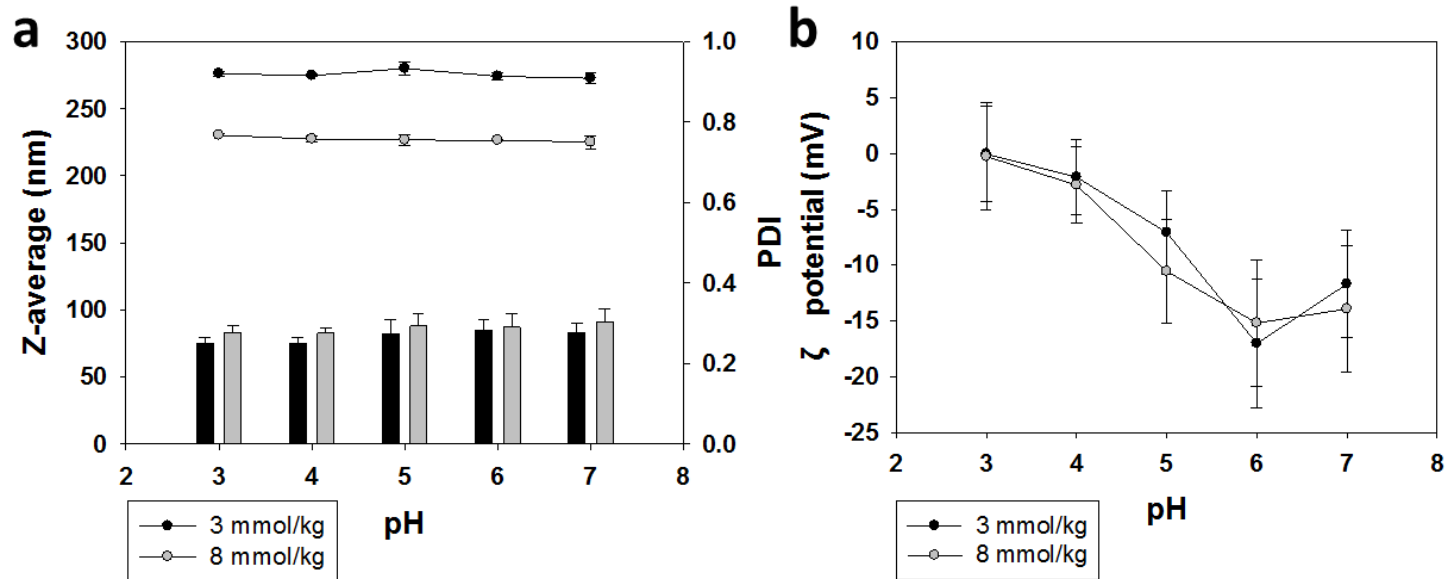


Figure 11. Values for (a) z-average and (b) ζ -potential of Brij S100-stabilized solid lipid nanoparticles at pH 3-7 (25 °C).

In the DSC melting thermogram, the SLNs made under the experimental conditions showed more dominant formation of α or β' -form crystal than β -form crystal. It is well known that surface active species affect polymorphism and crystallization temperature of triglyceride nanoparticles (Aronhime, Sarig, & Garti, 1988; Bunjes, Koch, & Westesen, 2002, 2003). These effects are largely influenced by the molecular structure of the surface active entity (Bunjes et al., 2003). Recent studies have shown that the presence of liquid polysorbate surfactant (Tween 80) has a greater effect on the shape of the DSC melting curve than when only tristearin is present. When Tween 80 was used to make tristearin particles, the peak temperature and liquid crystalline transition in the DSC thermogram changed (Ioanna Zafeiri, Norton, Smith, Norton, & Spyropoulos, 2017). This interaction creates a complex crystalline structure, which can result in multiple melting events (Helgason, Awad, Kristbergsson, McClements, & Weiss, 2009).

The tendency of increasing the formation of α or β' -form than β -form crystal was observed as the concentration of emulsifier used increased. Recent studies have shown that SLNs made with 0.8% Tween 80 form a higher fraction of β -form crystals than SLNs made with 1.2% Tween 80. And SLNs made with 2% Tween 80 showed higher ratio of α -form crystal and lower rate of β -form crystal than SLNs made with 1.2% Tween 80. A high concentration

of Tween 80 means that the alkyl tail of the emulsifier is packed more tightly with the oil-water interface, creating a more rigid structure. The crystal structure becomes more intricate and the suspension exhibits a more complex melting pattern (T Helgason et al., 2009; Ioanna Zafeiri et al., 2017). In addition, low-melting surfactant such as Tween 80 tends to promote the formation of β' or β -form crystal in tripalmitin solid lipid nanoparticles (SLNs) suspension compared to high-melting surfactant such as Tween 60. The tail layer of the high-melting surfactant acts as a template for nucleation and then the crystallization of the lipid matrix forms an α -subcell crystal form (Thrandur Helgason et al., 2009). Thus, the tendency observed in results is generally consistent with known research results.

In the DSC melting thermogram, the melting peak of α -form crystal appeared at 51 °C and 53 °C for SLNs stabilized with Tween 60 (Fig 13), 46 °C and 53 °C for Brij S20 (Fig 14) and 47 °C and 53 °C for Brij S100 (Fig 15). The results show that the melting peak of α -form crystal is split into two regions. This trend is explained in a previous study of emulsion using alkanes. The emulsifier is mainly located on the surface of the emulsion, where melting of the emulsion surface and melting of the core have different peaks. This is because the core of the emulsion is a relatively pure lipid and the hydrophobic tail of the emulsifier acts as an impurity on the surface of the emulsion. This

tendency increases as the hydrophobic tail of the emulsifier resembles the size of the lipid molecule and the droplet size becomes smaller (Gülseren & Coupland, 2008). The subsequent β' and β -form crystal melting peaks were 62 °C and 70 °C, respectively. This is in agreement with the results of previous experiments in which the first peak means α -polymorph of ~ 54 °C, the peak of ~ 63.5 °C is β' -form, and finally the peak of ~ 70 °C is stable β -form (Lavigne, Bourgaux, & Ollivon, 1993) (Fig 12).

As the SLNs are prepared, the emulsifier can be embedded into the interior as well as outside. This phenomenon also affects the crystal form, with Brij S20-stabilized SLNs having fewer β' - and more α -form crystal portions than Tween 60-stabilized SLNs. This is because the Tween 60 occupies a larger space due to the structural difference, and thus the penetration into the interior is relatively less. Brij S100 is also less invasive to the interior than the Brij S20 due to its large volume and relatively high hydrophilicity, and thus has relatively fewer α/β' - and more β -form crystals.

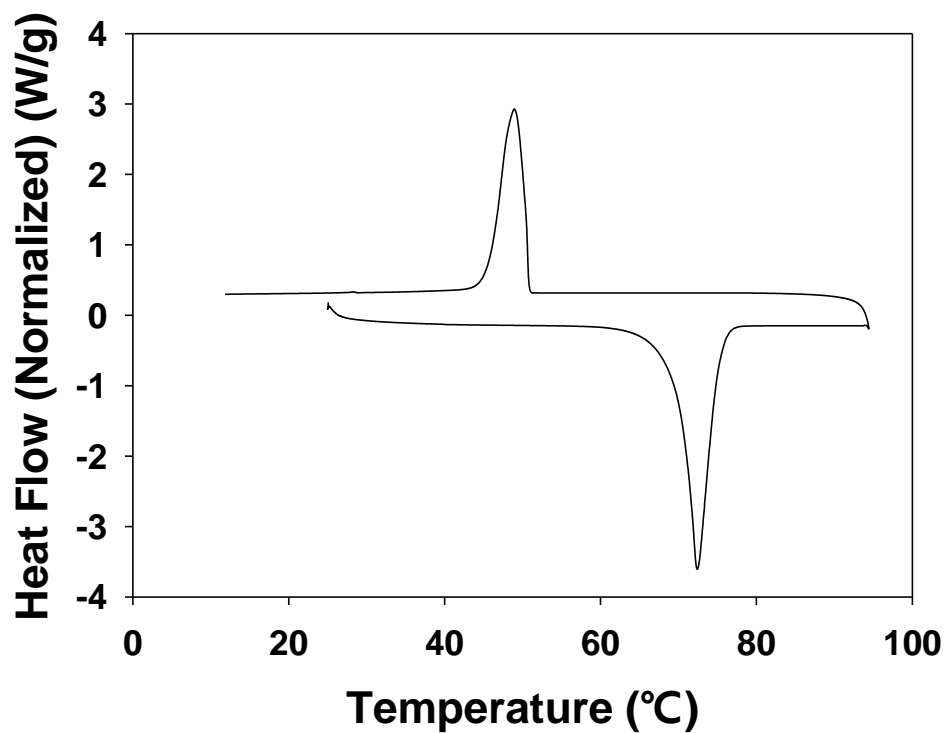


Figure 12. Melting (bottom line) and crystallization (top line) thermograms of bulk tristearin in the differential scanning calorimetry.

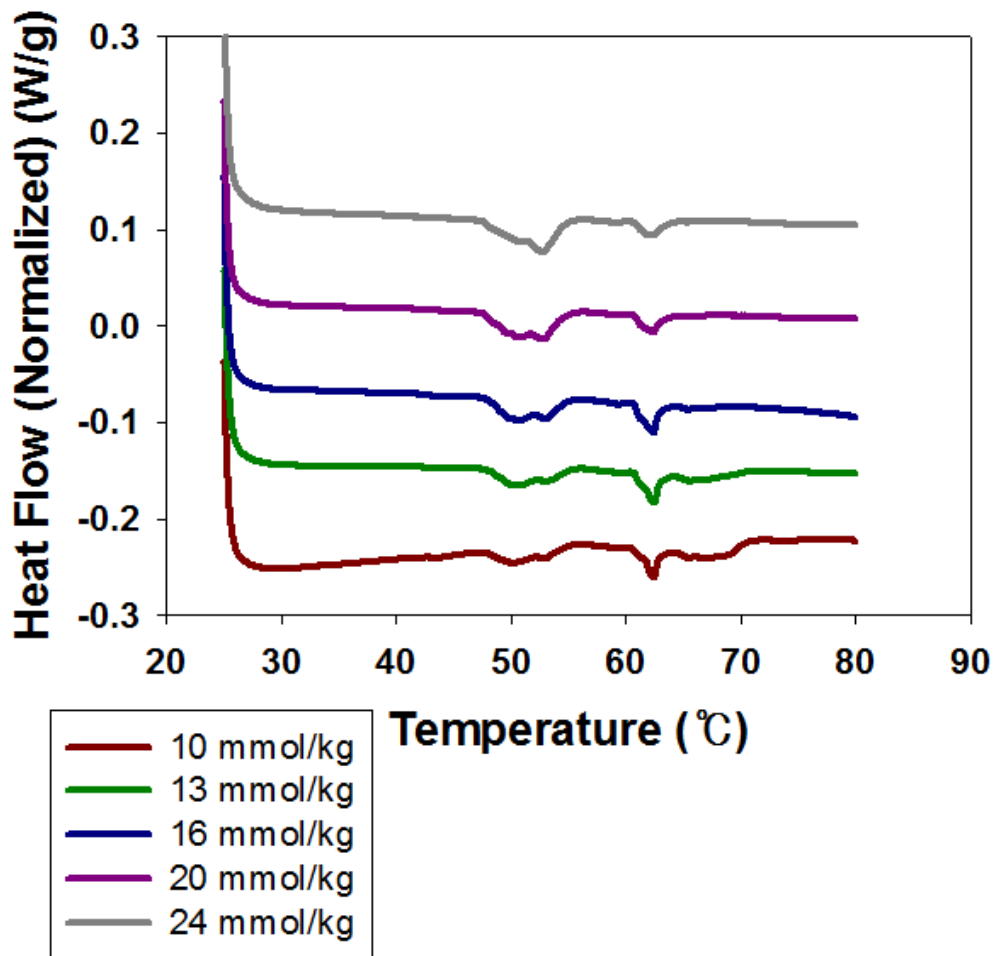


Figure 13. Melting thermograms of Tween 60-stabilized solid lipid nanoparticles in the differential scanning calorimetry.

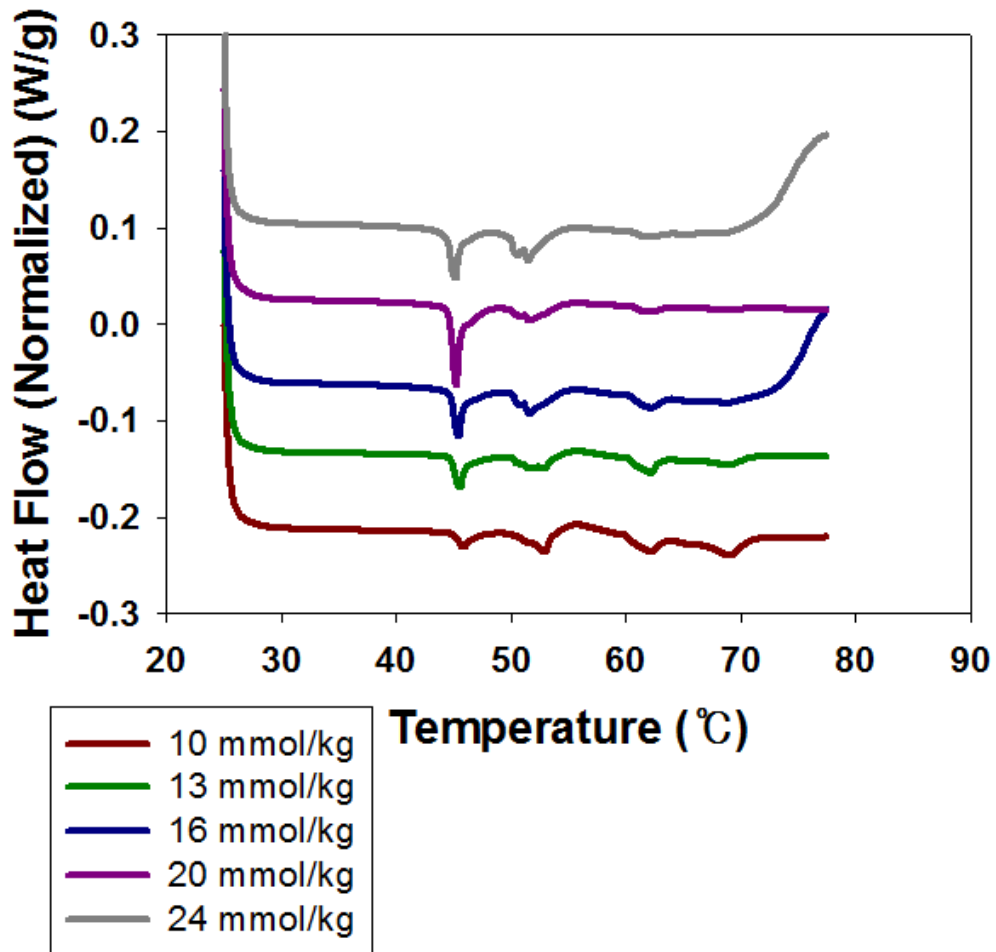


Figure 14. Melting thermograms of Brij S20-stabilized solid lipid nanoparticles in the differential scanning calorimetry.

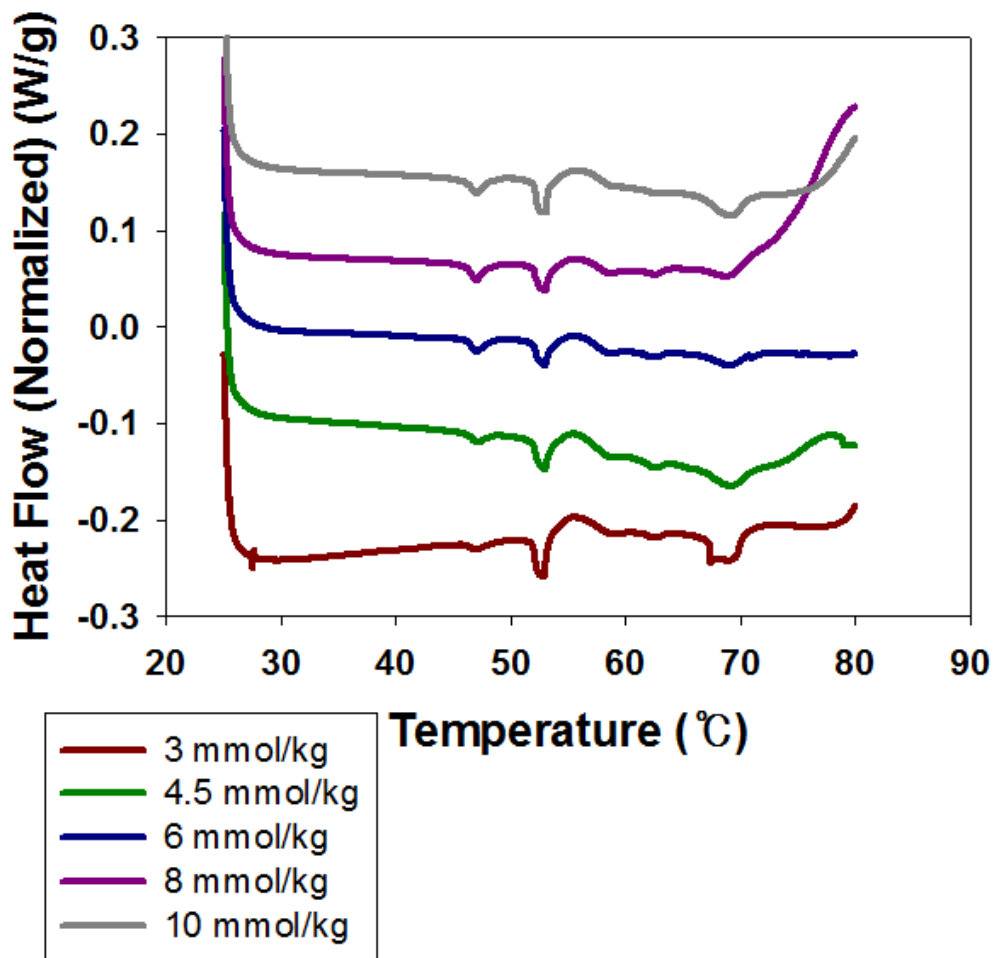


Figure 15. Melting thermograms of Brij S100-stabilized solid lipid nanoparticles in the differential scanning calorimetry.

Transmission electron microscopy (TEM) was used to observe the size and morphology of SLNs (Fig 16, 17, 18). In TEM observation, SLNs showed a good agreement when compared with size distribution measured by dynamic light scattering method. In addition, it was confirmed that even the SLNs made with the lowest concentration of emulsifier used in the experiment is almost spherical and therefore suitable for the analysis by the gel-trap method.

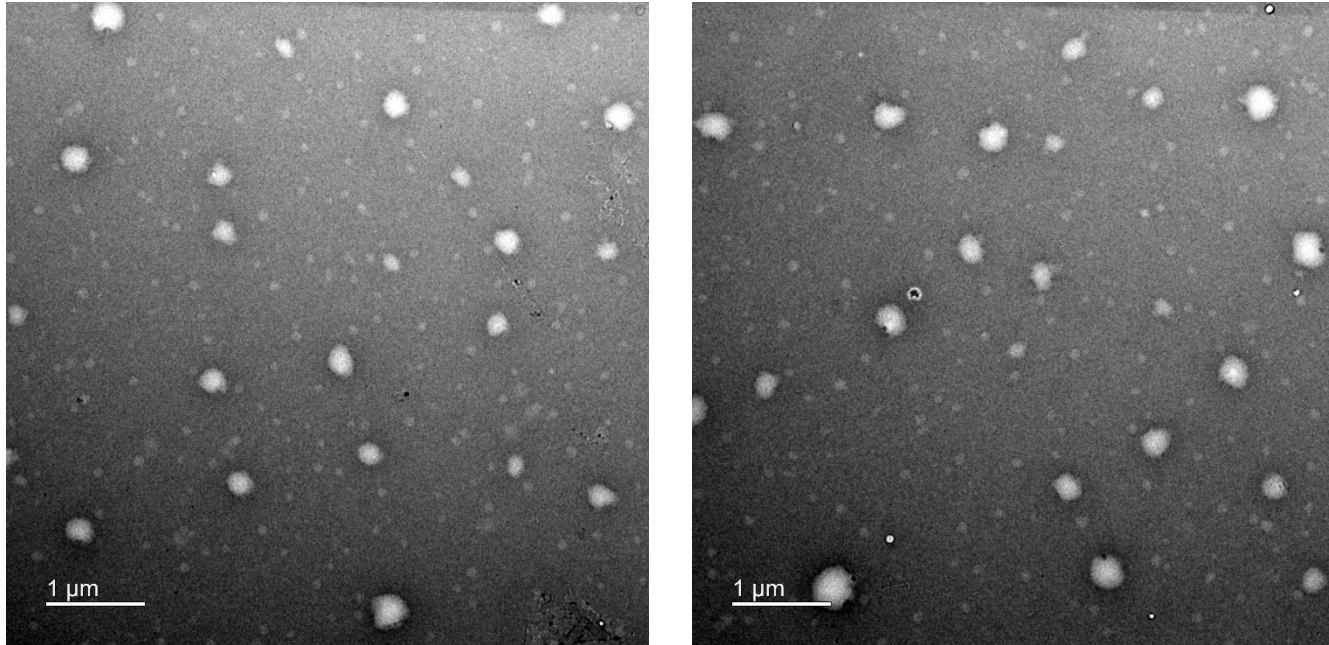


Figure 16. Transmission electron micrographs of the solid lipid nanoparticles stabilized with 10 mmol/kg of Tween 60.

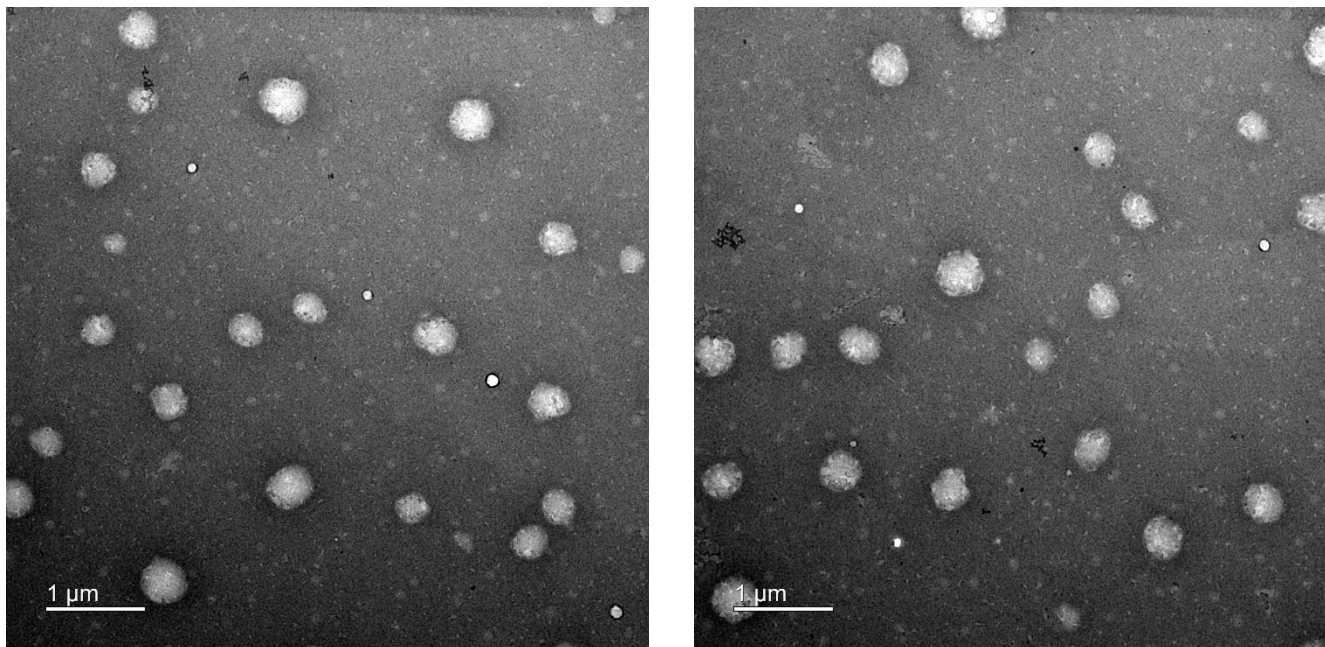


Figure 17. Transmission electron micrographs of the solid lipid nanoparticles stabilized with 10 mmol/kg of Brij S20.

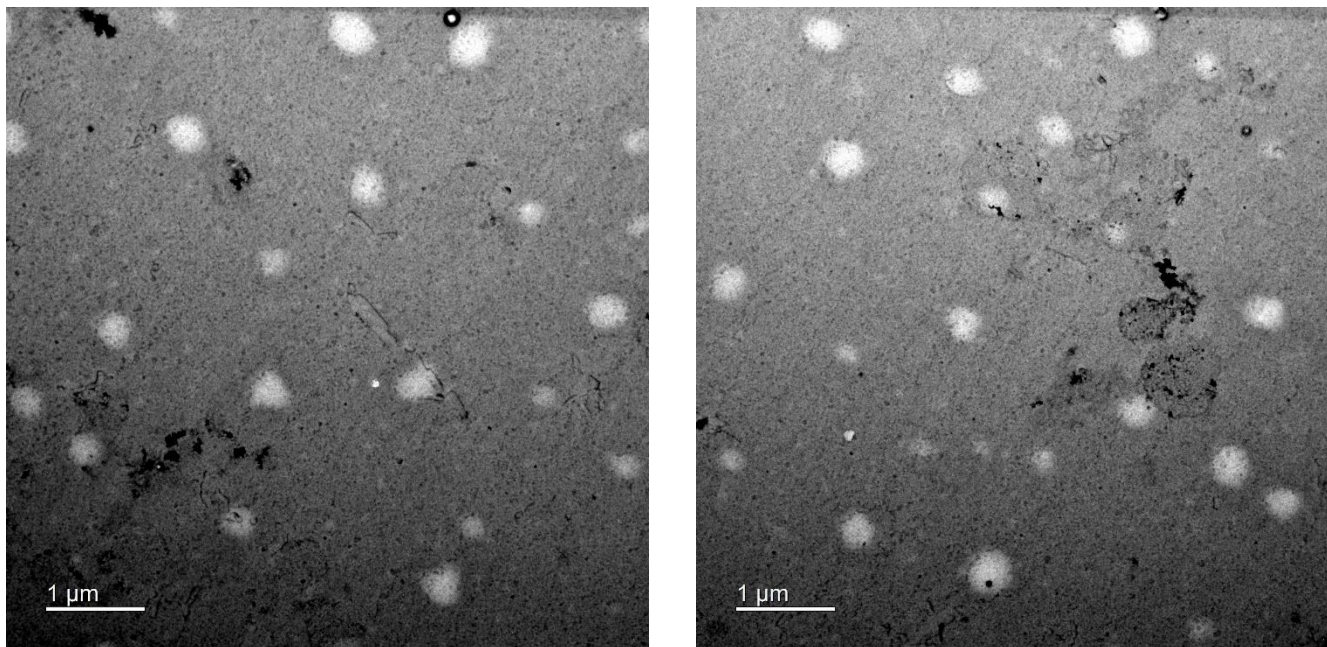


Figure 18. Transmission electron micrographs of the solid lipid nanoparticles stabilized with 3 mmol/kg of Brij S100.

The modified gel-trap method was used to measure the contact angle at the oil-water interface of the SLNs (Paunov, 2003). To minimize the effect of free emulsifier on SLNs dispersion, dialyzed SLNs were used to measure contact angle and to make Pickering emulsion. Over 63.8-92.6 % of free emulsifier was removed by dialysis.

Height of the particles was measured except for the particles which deviated greatly from the size distribution on the AFM image (Fig 19, 20, 21). The contact angles were calculated from the observed height of 14-34 particles and z-average values (Fig 22).

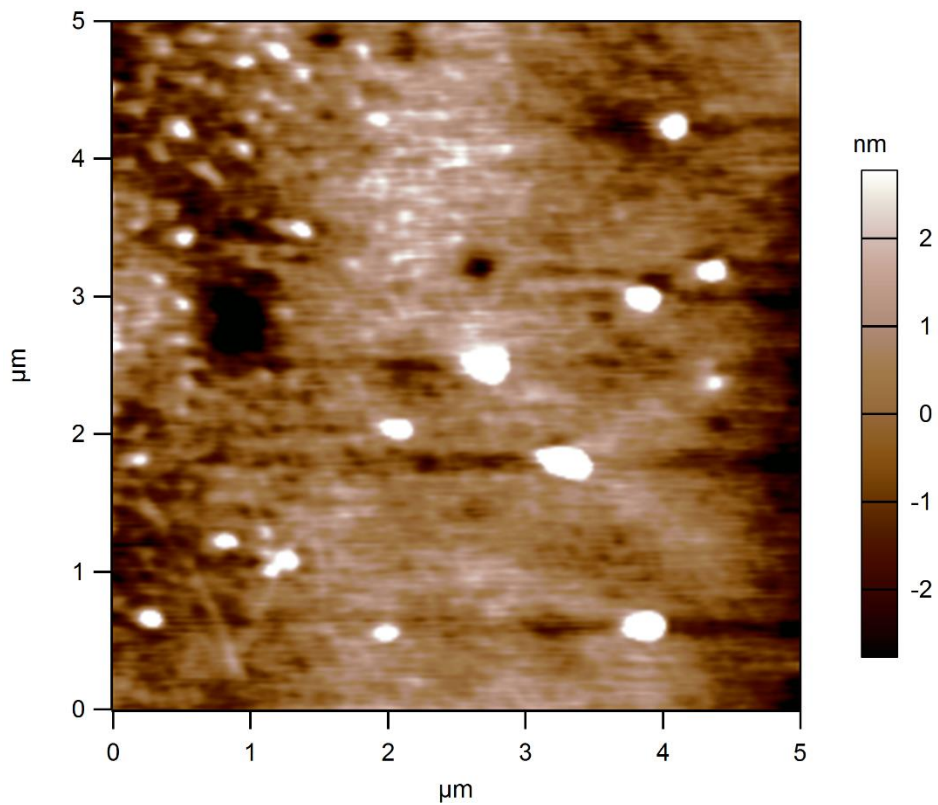


Figure 19. Atomic force micrograph of the polydimethylsiloxane-embedded solid lipid nanoparticles stabilized with 10 mmol/kg of Tween 60.

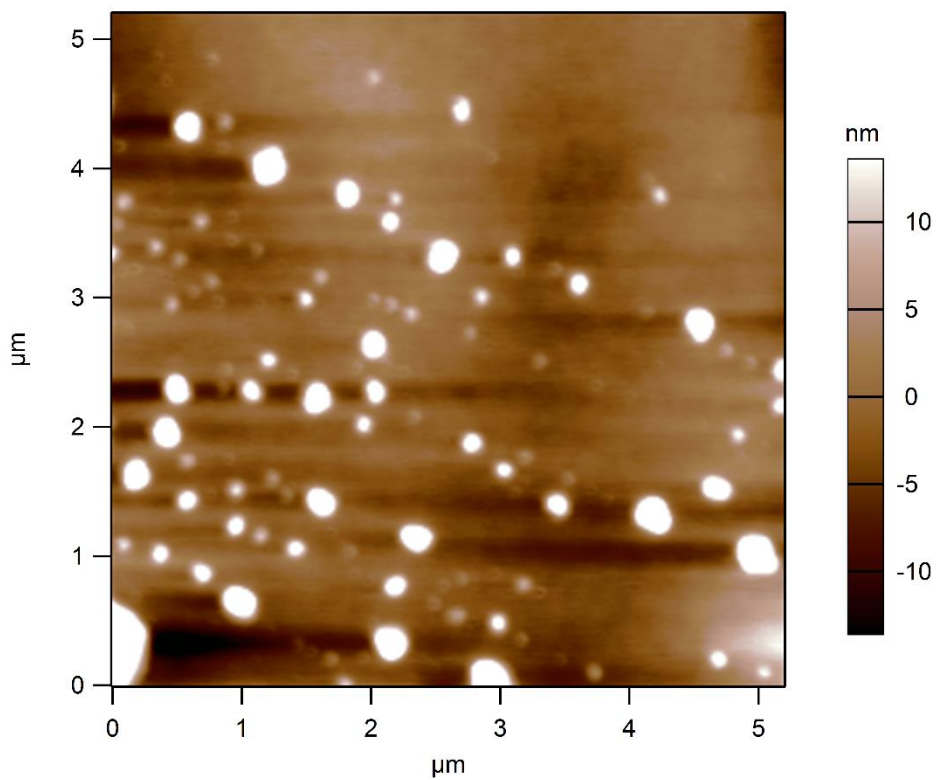


Figure 20. Atomic force micrograph of the polydimethylsiloxane-embedded solid lipid nanoparticles stabilized with 10 mmol/kg of Brij S20.

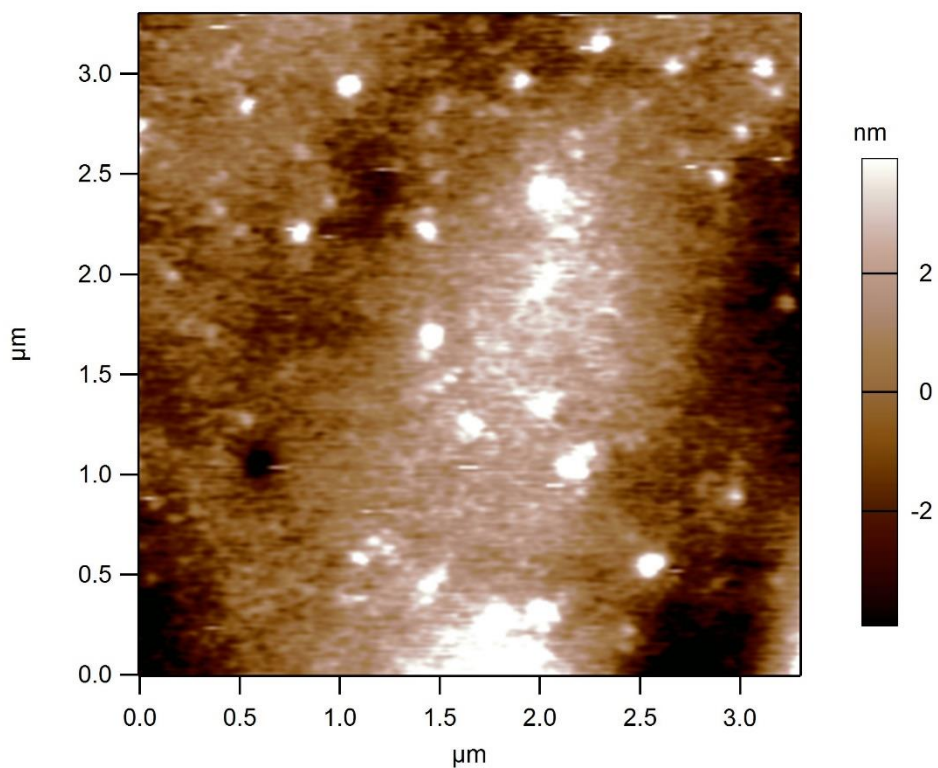


Figure 21. Atomic force micrograph of the polydimethylsiloxane-embedded solid lipid nanoparticles stabilized with 3 mmol/kg of Brij S100.

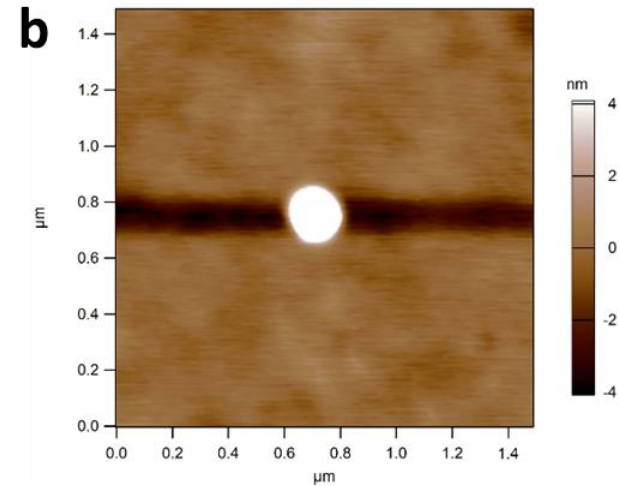
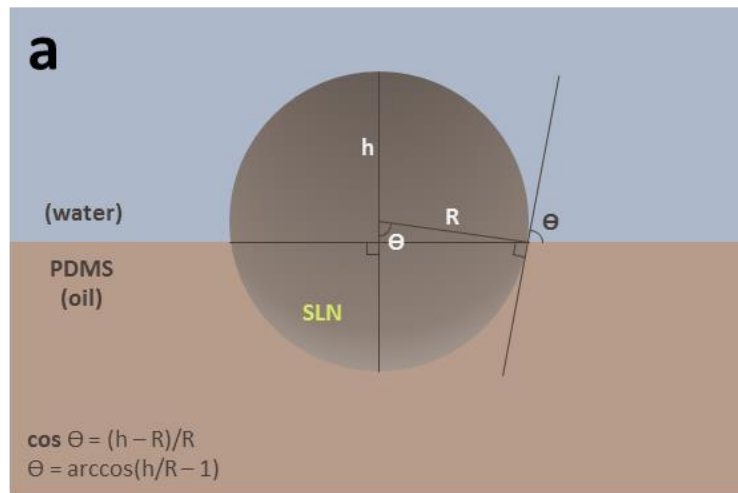


Figure 22. (a) A schematic representation of calculating contact angle of solid lipid nanoparticles embedded at the interface. (b) The interface-embedded SLNs stabilized with 10 mmol/kg of Brij S20.

Surface load value increased with increasing concentration of emulsifier in each SLNs-stabilized with three emulsifiers. Likewise, for all three emulsifiers used, α -form crystal tended to increase as the concentration of emulsifier increased, and the contact angle tended to decrease accordingly (Fig 23, 24, 25). The SLN contact angle at the saturating concentration of the emulsifiers used in the experiment was about 140, 135, and 150 ° in Tween 60, Brij S20, and Brij S100, respectively.

Tween 60 occupies a larger space due to the structural differences from the Brij S20 and thus has a relatively lower surface load. Contact angle also showed a lower tendency for Brij S20-stabilized SLNs at saturating concentrations than for Tween 60-stabilized SLNs. Brij S100-stabilized SLNs showed a lower contact angle despite lower α -form crystal and surface load compared to Brij S20-stabilized SLNs. This may be attributed to the longer hydrophilic PEG chain of Brij S100, which conferred greater hydrophilicity on SLNs. However, 10 mmol/kg Brij S100-stabilized SLNs showed a tendency to increase contact angle compared to SLNs at a concentration lower than 10 mmol/kg, even though surface load was increased.

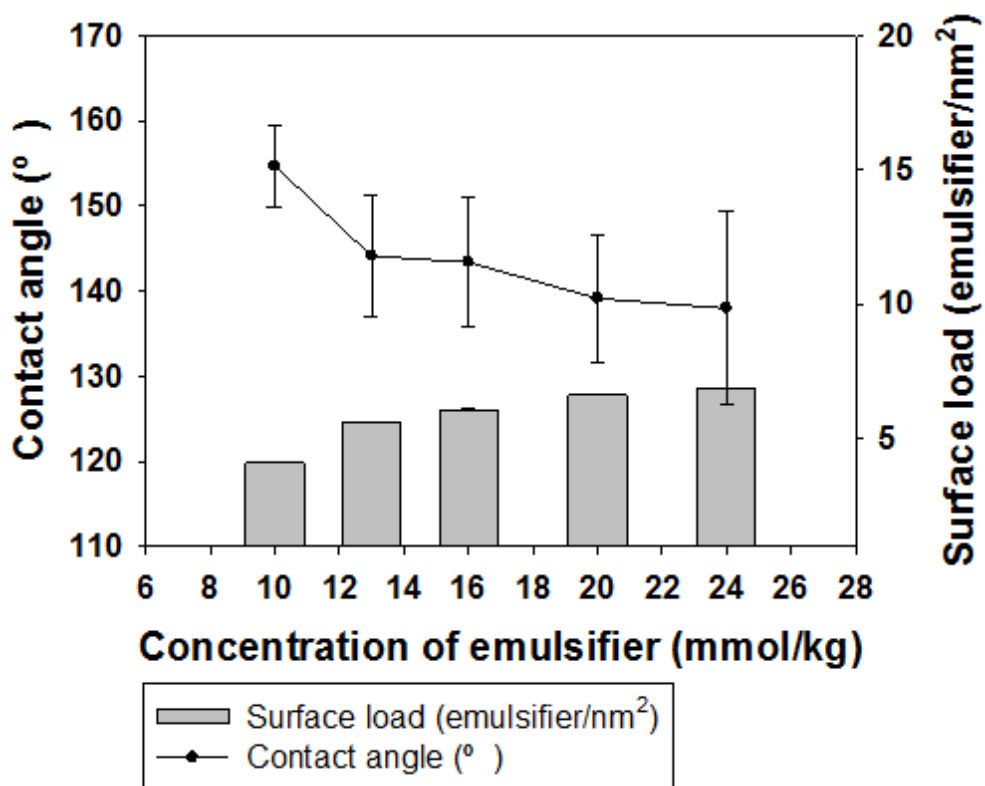


Figure 23. Contact angle of Tween 60-stabilized solid lipid nanoparticles (SLNs) in the oil-water interface, and surface load of the SLNs.

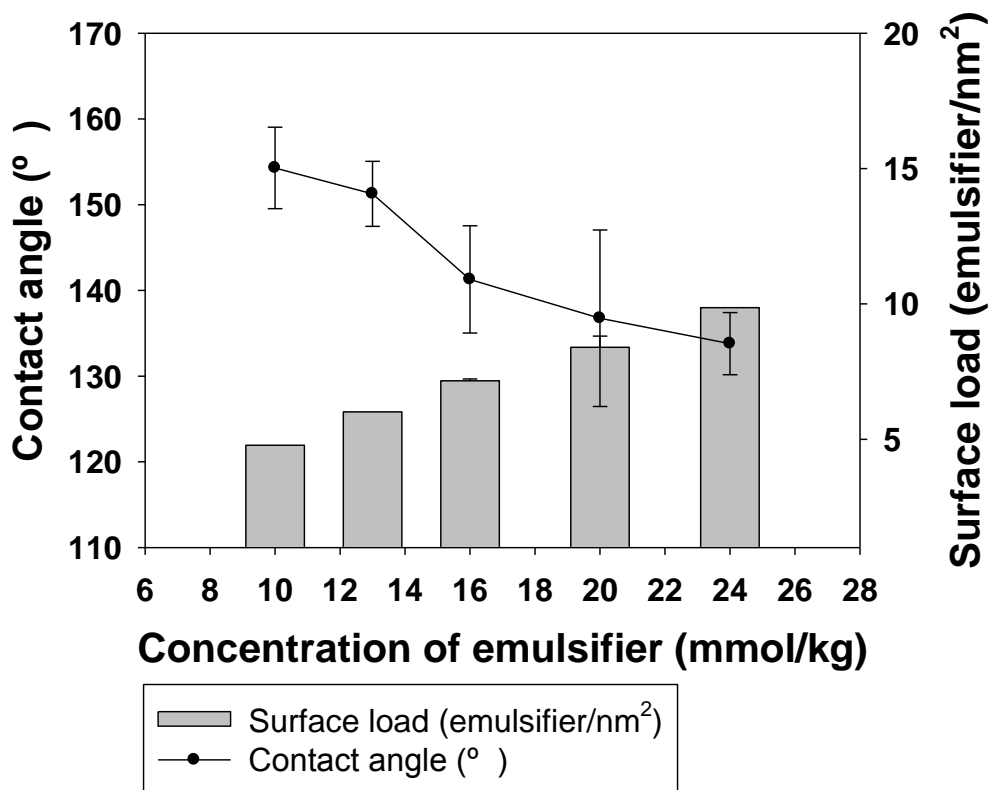


Figure 24. Contact angle of Brij S20-stabilized solid lipid nanoparticles (SLNs) in the oil-water interface, and surface load of the SLNs.

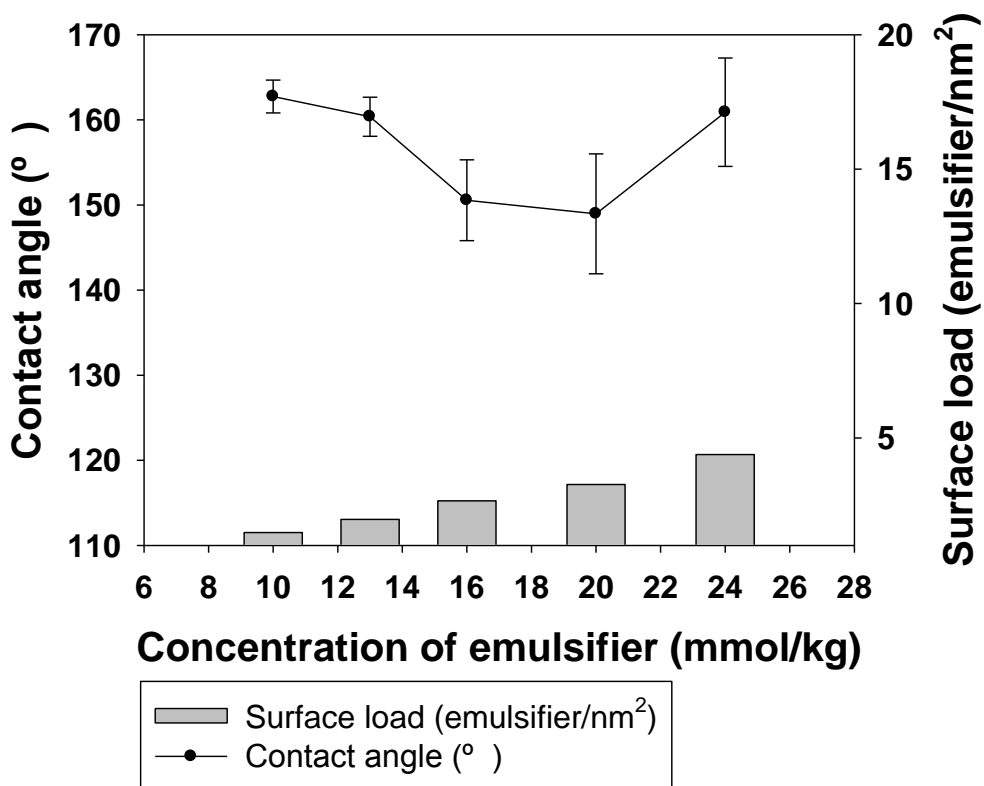


Figure 25. Contact angle of Brij S100-stabilized solid lipid nanoparticles (SLNs) in the oil-water interface, and surface load of the SLNs.

These results suggest that the contact angle of the SLNs is affected by the surface load of the emulsifier, but the crystal form of the SLNs has a stronger influence. Since all the emulsifiers used in the experiment saturate near the maximum concentration set, it is considered impossible to lower the contact angle using the emulsifier.

3.2. Preparation and characteristics of the SLNs-stabilized emulsions

To characterize the emulsions stabilized with SLNs, emulsion was prepared with 10 wt% canola oil. To minimize the heat-induced melting or aggregation of SLNs, an emulsion was formed in a jacket beaker at 2 °C. In order to confirm that the emulsion was stabilized by SLNs rather than the free emulsifier remaining in the SLNs dispersion, free emulsifiers were removed through dialysis.

Furthermore, the state of the emulsifier used to stabilize the emulsion was analyzed. To determine this, the amount of free emulsifier and canola oil used in the Pickering emulsion, and the measured $D_{3,2}$ value of Pickering emulsion were used for measurement. The emulsifier which stabilizes Pickering emulsion in the state attached to SLNs is expressed as “bound”. The

free emulsifier that exists in SLNs dispersion and stabilizes Pickering emulsion is expressed as “unbound”. The free emulsifier that exists in SLNs dispersion and stabilizes Pickering emulsion is expressed as “unbound”. In this experiment, the ratio of the bound and the total emulsifier used was expressed as the bound ratio. From these results, it was found that the Pickering emulsion with the ratio of 95% or more was stabilized by the SLNs rather than the free emulsifier. (Table 1).

Table 1. The amount of the Pickering emulsion-covering emulsifiers bound and unbound on the surface of the solid lipid nanoparticles (SLNs)

	Tween 60 ^a (mmol/kg)					Brij S20 ^b (mmol/kg)					Brij S100 ^c (mmol/kg)				
	10	13	16	20	24	10	13	16	20	24	3	4.5	6	8	10
Bound ^d (emulsifier/nm ²)	2.80	3.78	4.16	5.04	5.63	3.17	3.43	4.30	5.10	5.85	0.60	0.97	1.27	2.05	2.02
Unbound ^e (emulsifier/nm ²)	0.05	0.09	0.13	0.25	0.27	0.02	0.03	0.08	0.13	0.12	0.02	0.02	0.04	0.09	0.08
Bound ratio	0.98	0.98	0.97	0.95	0.95	0.99	0.99	0.98	0.97	0.98	0.97	0.98	0.97	0.96	0.96

SLNs stabilized with ^a Tween60, ^b Brij S20, and ^c Brij S100; the emulsifier which is attached to SLNs and stabilizes the Pickering emulsion is expressed as ^d bound. The emulsifier that remains as a free emulsifier in the SLNs dispersion and stabilizes the Pickering emulsion is expressed as ^e unbound. The number of emulsifiers per unit area of the Pickering emulsion is expressed in terms of the number of molecules, and the ratio of bound to unbound is also shown at the bottom.

For further analysis, emulsion was formed by hand shaking with reference to the method in the previous study (Schröder et al., 2017). In this experiment, the stability of the emulsion prepared with SLNs at the saturated concentration was found to be the highest, so the emulsion for the analysis using polarized microscopy was formed by using SLNs of saturated concentration. The SLNs-stabilized emulsion was found to have a distinct and thick interface (Fig 26, 27, 28). This suggests that the emulsion is stabilized by SLNs rather than free emulsifier in SLNs dispersion and SLNs maintain crystallinity at the oil-water interface. Under polarized microscopy, it was observed that a significant fraction of droplets retained a non-spherical shape. This seems to be due to the fact that SLNs are strongly attached to the oil-water interface and forms a strong interfacial network to prevent surface tension caused by shape relaxation of emulsion droplets (Richtering, 2012).

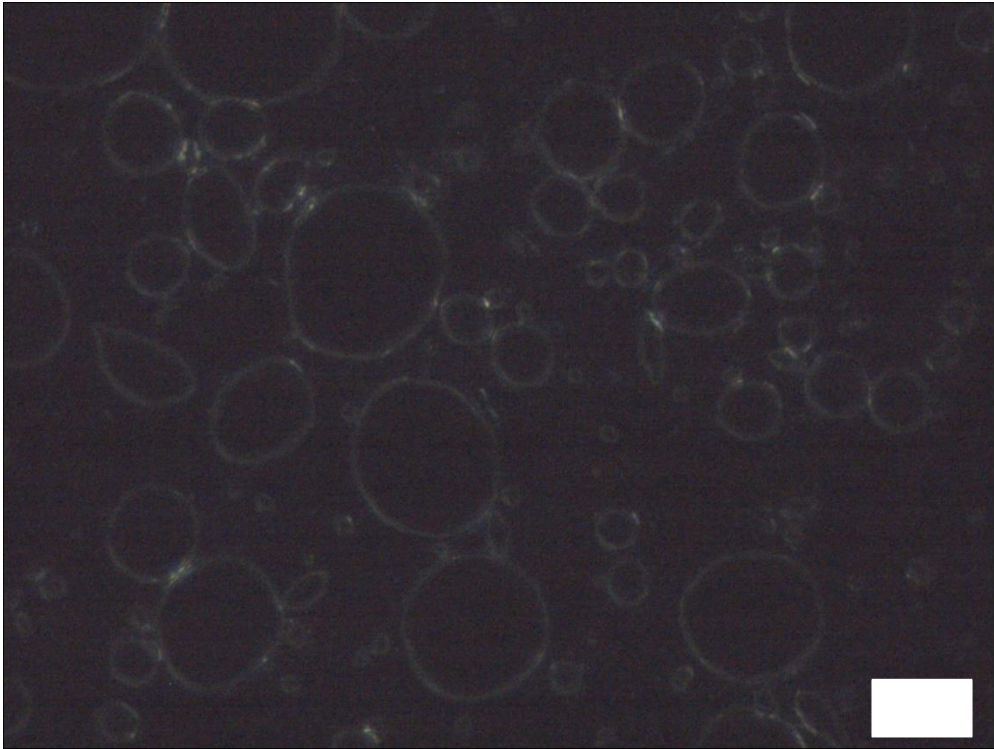


Figure 26. Polarized light micrograph of the hand-shaking emulsions prepared with 1 wt% of the Tween 60 (24 mmol/kg)-stabilized solid lipid nanoparticles and 10 wt% of canola oil (bar, 20 μm).

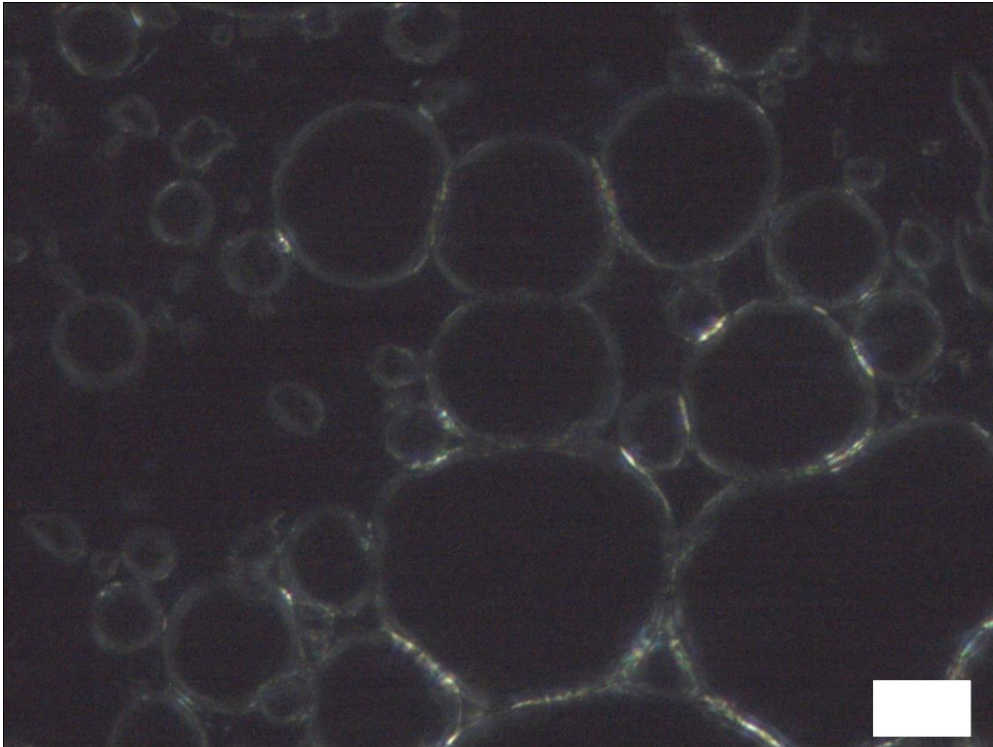


Figure 27. Polarized light micrograph of the hand-shaking emulsions prepared with 1 wt% of the Brij S20 (24 mmol/kg)-stabilized solid lipid nanoparticles and 10 wt% of canola oil (bar, 20 μm).

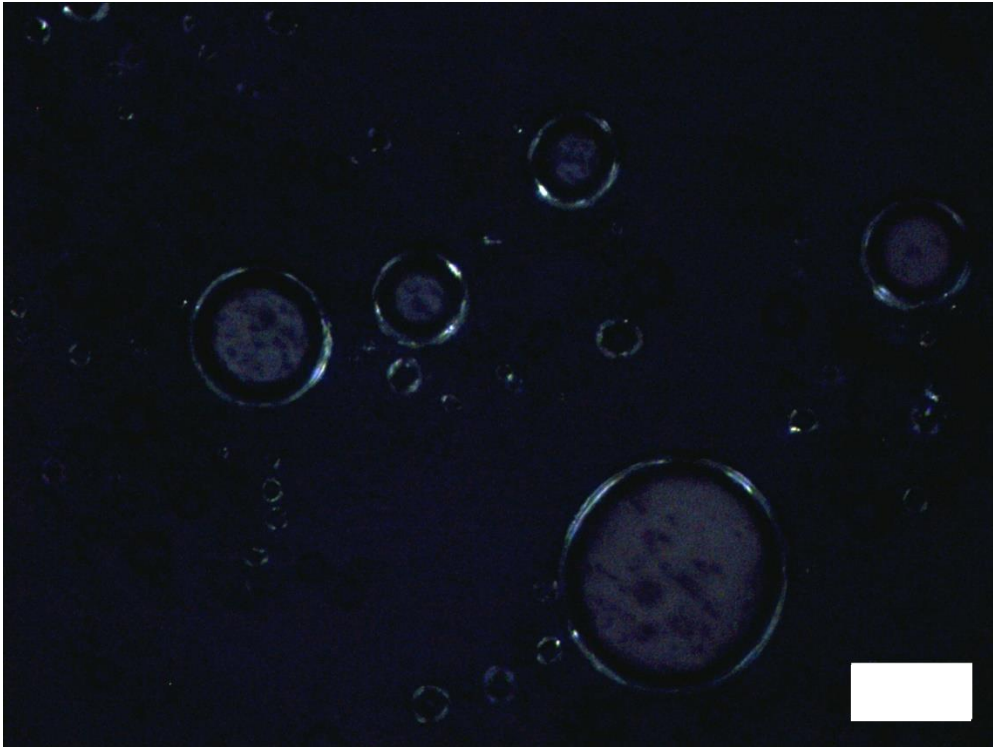


Figure 28. Polarized light micrograph of the hand-shaking emulsions prepared with 1 wt% of the Brij S100 (8 mmol/kg)-stabilized solid lipid nanoparticles and 10 wt% of canola oil (bar, 50 μm).

The storage stability of the prepared emulsion was evaluated. The droplet size of emulsion made using SLNs stabilized with 10 mmol/kg Tween 60 increased during the storage period. This is because the contact angle of the SLNs is too large to stabilize the oil-in-water emulsion and thus coalescence is considered to have occurred.

On the other hand, emulsion prepared using SLNs stabilized with 24 mmol/kg Tween 60 maintained a constant droplet size distribution even after a long storage period. In this case, it is considered that SLNs give strong stability to the droplet from the coalescence during storage period by forming a strong barrier in oil-water interface (Fig 29).

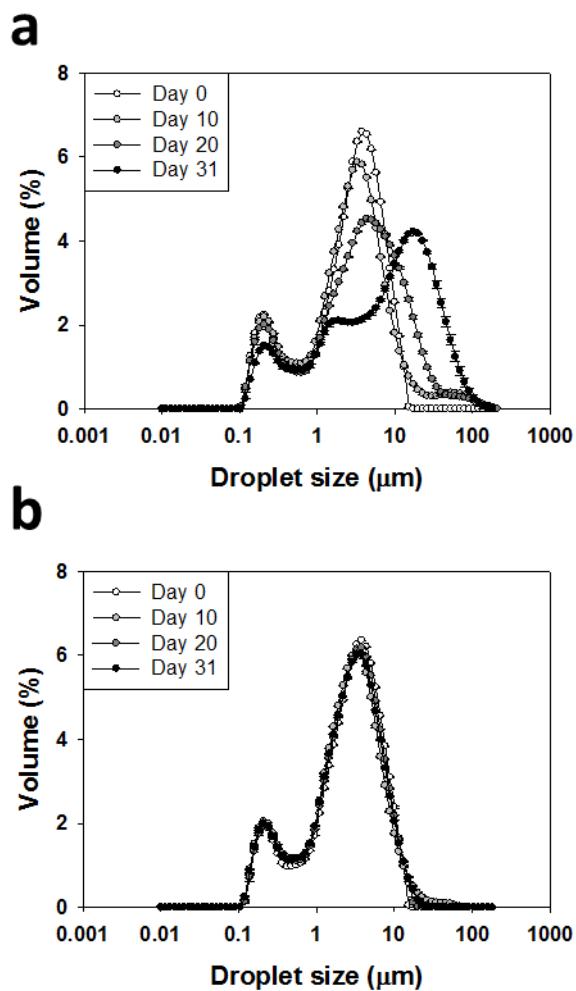


Figure 29. Particle size distribution of the emulsions prepared with 1 wt% of the Tween 60 ((a) 10 and (b) 24 mmol/kg)-stabilized solid lipid nanoparticles and 10 wt% canola oil after 0, 10, 20 and 31 day-storage.

Emulsions prepared using SLNs stabilized with 10 mmol/kg Brij S20 showed that the droplet size distribution tended to be pulled forward as the storage period increased. In this case, an irreversible lump was formed in the upper part of the emulsion during the storage period.

This suggests that the contact angle of SLNs is too large to stabilize the oil-in-water emulsion and is therefore vulnerable to coalescence same as the emulsion prepared with Tween 60-stabilized SLNs. In addition, the negative ζ -potential value of Brij S20-stabilized SLNs was much smaller than that of SLNs stabilized with the same 10 mmol/kg Tween 60, suggesting that the stability of prepared emulsion was lower than that of prepared with Tween 60-stabilized SLNs. Therefore, the emulsion made with Tween 60-stabilized SLNs retains its dispersed state even when the size increases, but the emulsion made of Brij S20-stabilized SLNs appears to have formed a lump.

When the droplet size is relatively large, rapid creaming occurs. In this process, unstable large oil droplets are rapidly destabilized through processes such as coalescence and flocculation. Unstable and large oil droplets form an irreversible lump through this process, and it is considered that the size distribution is pulled forward as a result.

The emulsion prepared using SLNs stabilized with 24 mmol/kg Brij S20 maintained a constant droplet size distribution even after a long storage period. In this case, it is considered that SLNs give strong stability to the droplet from the coalescence during storage period by forming a strong barrier in oil-water interface. In this experiment, the stability of emulsion stabilized with SLNs increases as the contact angle decreases. However, if the negative value of ζ -potential is too low, the stability of the emulsion may be lowered. It is considered that the SLNs covering the emulsion is not sufficient to provide sufficient dispersibility between the droplets (Fig 30).

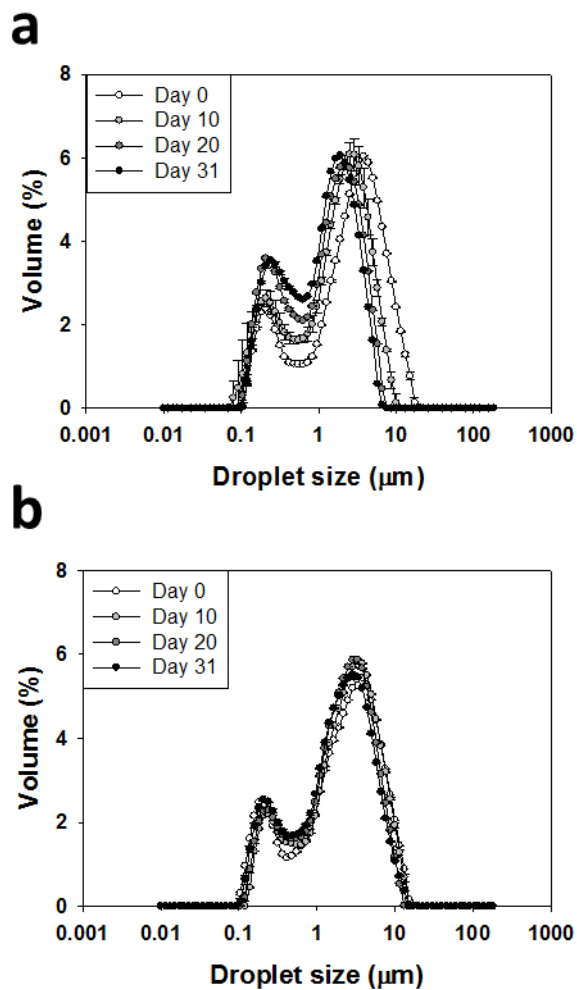


Figure 30. Particle size distribution of the emulsions prepared with 1 wt% of the Brij S20 ((a) 10 and (b) 24 mmol/kg)-stabilized solid lipid nanoparticles and 10 wt% canola oil after 0, 10, 20 and 31 day-storage.

Emulsions made using SLNs stabilized with 3 mmol/kg Brij S100 showed a droplet size distribution tendency to pull forward slightly as the storage period increased, as did emulsions stabilized with Brij S20 SLNs. In this case, during storage, a little lump was formed in the upper part of the emulsion. SLNs stabilized with a 3 mmol/kg of Brij S100 has a relatively large negative value of ζ -potential, but has a larger contact angle and higher hydrophobicity than SLNs-stabilized with 10 mmol/kg Tween 60 or Brij S20.

For this reason, the prepared emulsion is considered to be unstable during storage. However, SLNs stabilized with a 10 mmol/kg Brij S20 forms a more unstable emulsion compared to SLNs stabilized with 3 mmol/kg Brij S100, even with a lower contact angle. This tendency is attributed to the fact that SLNs stabilized by Brij S100 has a large negative value of ζ -potential and therefore SLNs give higher stability by providing dispersibility to emulsion.

Emulsions of SLNs stabilized with Brij S100 at 8 mmol / kg maintained their stability even with increasing storage period. SLNs stabilized with high concentration of Brij S100 has a larger contact angle value than SLNs stabilized with high concentration Tween 60 or Brij S20. However, SLNs stabilized by Brij S100 has a relatively large negative value of ζ -potential, which is considered to provide sufficient stability by forming a

strong barrier and providing dispersibility at the oil-water interface of the emulsion droplet (Fig 31).

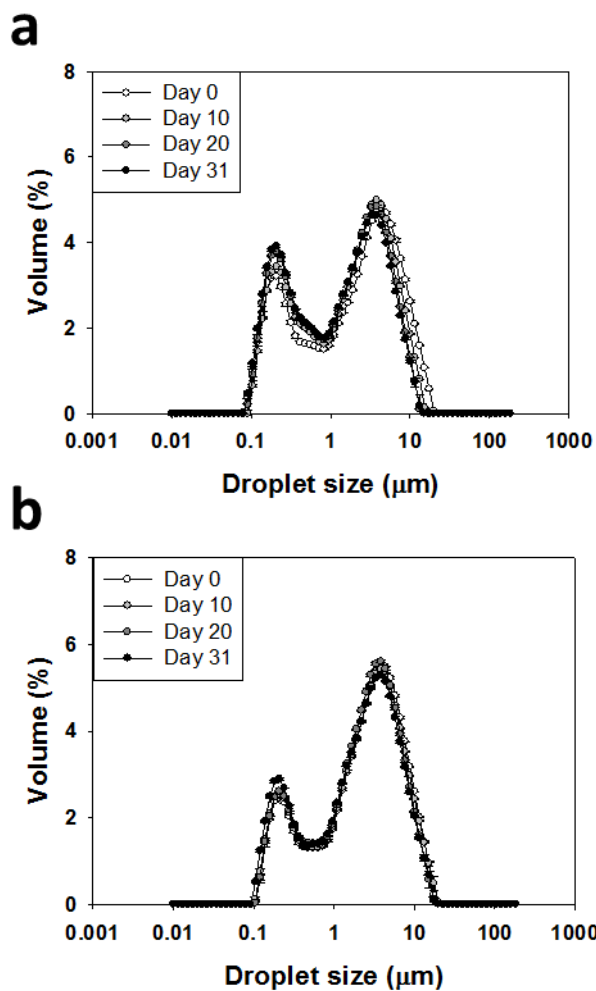


Figure 31. Particle size distribution of the emulsions prepared with 1 wt% of the Brij S100 ((a) 3 and (b) 8 mmol/kg)-stabilized solid lipid nanoparticles and 10 wt% canola oil after 0, 10, 20 and 31 day-storage.

IV. CONCLUSIONS

In this study, the basic research for utilizing solid lipid nanoparticles as a Pickering stabilizer was conducted. Three kinds of PEGylated emulsifiers were used and the effects of the emulsifier concentrations and properties were studied. The crystal form and surface load seem to affect the contact angle of SLNs, but it is considered that the crystal form of lipid plays a major role in the concentration of emulsifier above a certain level. As the formation of α , β' -form crystals increased and the surface load increased, the hydrophilicity of SLNs increased. The contact angles of the SLNs at the concentration of the emulsifier saturates were 140, 135, and 150 ° at Tween 60, Brij S20, and Brij S100, respectively. The oil-in-water emulsion was prepared using sole SLNs by removing the free emulsifier through dialysis. It has been confirmed that SLNs effectively stabilize oil-in-water emulsion through high bond energy even when it is relatively hydrophobic. When SLNs made with saturated concentration of emulsifier was used as a Pickering stabilizer, it maintained a constant size distribution for more than 4 weeks. In addition, a more stable emulsion was formed when the negative ζ -potential value of SLNs were large. When the negative ζ -potential value of SLNs are large, it is considered that

SLNs improve stability of prepared emulsion by providing dispersibility. The results of this study can be used as versatile data in further studies to apply SLNs as Pickering stabilizer.

V. REFERENCES

- Aronhime, J. S., Sarig, S., & Garti, N. (1988). Dynamic control of polymorphic transformation in triglycerides by surfactants: The button syndrome. *Journal of the American Oil Chemists' Society*, 65(7), 1144-1150.
- Aveyard, R., Binks, B. P., & Clint, J. H. (2003). Emulsions stabilised solely by colloidal particles. *Advances in Colloid and Interface Science*, 100-102, 503-546. doi:[https://doi.org/10.1016/S0001-8686\(02\)00069-6](https://doi.org/10.1016/S0001-8686(02)00069-6)
- Ban, C., Jo, M., Lim, S., & Choi, Y. J. (2018). Control of the gastrointestinal digestion of solid lipid nanoparticles using PEGylated emulsifiers. *Food chemistry*, 239, 442-452.
- Berton-Carabin, C. C., & Schroën, K. (2015). Pickering emulsions for food applications: background, trends, and challenges. *Annual review of food science and technology*, 6, 263-297.
- Binks, B. P., & Rocher, A. (2009). Effects of temperature on water-in-oil emulsions stabilised solely by wax microparticles. *Journal of Colloid and Interface Science*, 335(1), 94-104. doi:<https://doi.org/10.1016/j.jcis.2009.03.089>
- Bunjes, H., Koch, M. H., & Westesen, K. (2002). Effects of surfactants on the crystallization and polymorphism of lipid nanoparticles *Molecular Organisation on Interfaces* (pp. 7-10): Springer.
- Bunjes, H., Koch, M. H., & Westesen, K. (2003). Influence of emulsifiers on the crystallization of solid lipid nanoparticles. *Journal of*

- pharmaceutical sciences*, 92(7), 1509-1520.
- Dickinson, E. (2010). Food emulsions and foams: Stabilization by particles. *Current Opinion in Colloid & Interface Science*, 15(1), 40-49.
doi:<https://doi.org/10.1016/j.cocis.2009.11.001>
- Dickinson, E. (2012). Use of nanoparticles and microparticles in the formation and stabilization of food emulsions. *Trends in Food Science & Technology*, 24(1), 4-12.
- Finkle, P., Draper, H. D., & Hildebrand, J. H. (1923). The theory of emulsification1. *Journal of the American Chemical Society*, 45(12), 2780-2788.
- Frasch-Melnik, S., Norton, I. T., & Spyropoulos, F. (2010). Fat-crystal stabilised w/o emulsions for controlled salt release. *Journal of Food Engineering*, 98(4), 437-442.
- French, D. J., Brown, A. T., Schofield, A. B., Fowler, J., Taylor, P., & Clegg, P. S. (2016). The secret life of Pickering emulsions: particle exchange revealed using two colours of particle. *Scientific Reports*, 6, 31401.
doi:10.1038/srep31401
- Gülseren, İ., & Coupland, J. N. (2008). Surface melting in alkane emulsion droplets as affected by surfactant type. *Journal of the American Oil Chemists' Society*, 85(5), 413-419.
- Gupta, R., & Rousseau, D. (2012). Surface-active solid lipid nanoparticles as Pickering stabilizers for oil-in-water emulsions. *Food & function*, 3(3), 302-311.
- Helgason, T., Awad, T., Kristbergsson, K., McClements, D. J., & Weiss, J. (2009). Effect of surfactant surface coverage on formation of solid lipid nanoparticles (SLN). *Journal of Colloid and Interface Science*, 334(1), 75-81.

- Helgason, T., Awad, T. S., Kristbergsson, K., Decker, E. A., McClements, D. J., & Weiss, J. (2009). Impact of surfactant properties on oxidative stability of β -carotene encapsulated within solid lipid nanoparticles. *Journal of Agricultural and Food Chemistry*, 57(17), 8033-8040.
- Kotula, A. P., & Anna, S. L. (2012). Probing timescales for colloidal particle adsorption using slug bubbles in rectangular microchannels. *Soft Matter*, 8(41), 10759-10772.
- Lavigne, F., Bourgaux, C., & Ollivon, M. (1993). Phase transitions of saturated triglycerides. *Le Journal de Physique IV*, 3(C8), C8-137-C138-140.
- Leal-Calderon, F., & Schmitt, V. (2008). Solid-stabilized emulsions. *Current Opinion in Colloid & Interface Science*, 13(4), 217-227.
doi:<https://doi.org/10.1016/j.cocis.2007.09.005>
- McClements, D. J. (2015). *Food emulsions: principles, practices, and techniques*: CRC press.
- Monteillet, H., Workamp, M., Li, X., Schuur, B., Kleijn, J. M., Leermakers, F. A., & Sprakel, J. (2014). Multi-responsive ionic liquid emulsions stabilized by microgels. *Chemical communications*, 50(81), 12197-12200.
- Morris, V. J. (2011). Emerging roles of engineered nanomaterials in the food industry. *Trends in Biotechnology*, 29(10), 509-516.
doi:<https://doi.org/10.1016/j.tibtech.2011.04.010>
- Nagaoka, S., & Nakao, A. (1990). Clinical application of antithrombogenic hydrogel with long poly (ethylene oxide) chains. *Biomaterials*, 11(2), 119-121.
- Paunov, V. N. (2003). Novel method for determining the three-phase contact angle of colloid particles adsorbed at air– water and oil– water

- interfaces. *Langmuir*, 19(19), 7970-7976.
- Pawlik, A., Kurukji, D., Norton, I., & Spyropoulos, F. (2016). Food-grade Pickering emulsions stabilised with solid lipid particles. *Food & function*, 7(6), 2712-2721.
- Pichot, R., Spyropoulos, F., & Norton, I. T. (2009). Mixed-emulsifier stabilised emulsions: Investigation of the effect of monoolein and hydrophilic silica particle mixtures on the stability against coalescence. *Journal of Colloid and Interface Science*, 329(2), 284-291. doi:<https://doi.org/10.1016/j.jcis.2008.09.083>
- Pickering, S. U. (1907). Cxcvi.-emulsions. *J. Chem. Soc. Trans.*, 91, 2001-2021.
- Richtering, W. (2012). Responsive emulsions stabilized by stimuli-sensitive microgels: emulsions with special non-Pickering properties. *Langmuir*, 28(50), 17218-17229.
- Rousseau, D. (2000). Fat crystals and emulsion stability—a review. *Food Research International*, 33(1), 3-14.
- Rousseau, D. (2013). Trends in structuring edible emulsions with Pickering fat crystals. *Current Opinion in Colloid & Interface Science*, 18(4), 283-291.
- Schröder, A., Corstens, M. N., Ho, K. K., Schroën, K., & Berton- Carabin, C. C. (2018). Pickering Emulsions. *Emulsion- based Systems for Delivery of Food Active Compounds: Formation, Application, Health and Safety*, 29-67.
- Schröder, A., Sprakel, J., Schroën, K., & Berton-Carabin, C. C. (2017). Tailored microstructure of colloidal lipid particles for Pickering emulsions with tunable properties. *Soft Matter*, 13(17), 3190-3198.
- Thompson, K. L., Williams, M., & Armes, S. P. (2015). Colloidosomes:

Synthesis, properties and applications. *Journal of Colloid and Interface Science*, 447, 217-228.

doi:<https://doi.org/10.1016/j.jcis.2014.11.058>

Timgren, A., Rayner, M., Sjöö, M., & Dejmeek, P. (2011). Starch particles for food based Pickering emulsions. *Procedia Food Science*, 1, 95-103.

doi:<https://doi.org/10.1016/j.profoo.2011.09.016>

Zafeiri, I., Norton, J. E., Smith, P., Norton, I. T., & Spyropoulos, F. (2017). The role of surface active species in the fabrication and functionality of edible solid lipid particles. *Journal of Colloid and Interface Science*, 500, 228-240.

Zafeiri, I., Smith, P., Norton, I., & Spyropoulos, F. (2017). Fabrication, characterisation and stability of oil-in-water emulsions stabilised by solid lipid particles: the role of particle characteristics and emulsion microstructure upon Pickering functionality. *Food & function*, 8(7), 2583-2591.

Zhou, W., Cao, J., Liu, W., & Stoyanov, S. (2009). How Rigid Rods Self-Assemble at Curved Surfaces. *Angewandte Chemie International Edition*, 48(2), 378-381.

국 문 초 록

최근 고품지질나노입자를 피커링 안정제로서 사용하기 위한 많은 연구가 진행되고 있다. 고품지질나노입자는 식용이며 저렴하고 제작 과정이 간편한 장점이 있다. 또한 고품지질나노입자는 제작 조건에 따라 특성과 형태의 조절이 간편하다. 피커링 안정제로서 고품지질나노입자는 특성에 따라 수중 유적, 유중 수적 시스템 양쪽 모두에 적용이 가능하며 고품지질나노입자로 안정화된 에멀전은 일반적인 유화제로 안정화된 에멀전에 비하여 뛰어난 물리적 안정성을 가진다. 이번 연구에서 고품 지질 나노 입자를 안정화시키기 위해 필수적으로 필요한 유화제로 인해 부여되는 특성에 대한 연구를 진행하였다. Tween 60, Brij S20, Brij S100 3가지 유화제의 농도를 조절하고 고품 지질(트리스테아린)과 함께 고온에서 초음파 처리 방법을 이용해 고품지질나노입자를 제작하였다. 사용된 유화제의 농도가 높아짐에 따라 surface load와 α/β' -형태 결정의 형성이 증가하고 β -형태 결정이 감소하는 경향이 나타났다. 유화제에 의한 안정화 효과를 최소화하기 위하여 투석을 통해 잔여 유화제를 제거하고 접촉각을 측정하였다. 고품지질나노입자의 접촉각은 유화제의

surface load와 α/β' -형태 결정의 형성이 증가할수록, β -형태 결정이 줄어들수록 작아지는 경향이 나타났다. 유화제의 포화 농도에서 접촉각은 Tween 60, Brij S20, Brij S100에서 각각 140°, 135°, 150° 수준으로 나타났다. 또한 고행지질나노입자의 접촉각은 유화제의 surface load보다 형성되는 지질 결정 구조에 더 크게 영향을 받는 것으로 보인다. 고행지질나노입자로 안정화된 수중 유적 피커링 에멀전의 안정성도 평가되었다. 실험 조건에서 피커링 에멀전의 안정성은 고행지질나노입자의 접촉각이 작을수록, 제타 포텐셜 값이 클수록 높아지는 경향이 나타났다. 또한 각 유화제의 포화 농도에서 제작된 고행지질나노입자를 피커링 안정제로 사용하는 경우 4주 이상 일정한 입도 분포를 유지하여 높은 안정성을 나타내었다. 우리의 결과는 고행지질나노입자를 사용한 피커링 에멀전의 활용에 있어서 범용성있게 적용이 가능할 것이며 새로운 전달 시스템 제작에 있어 새로운 시각을 만들어줄 것이다.

주요어: 피커링 에멀전, 고행지질나노입자, 유화제, 접촉각, surface load

학번: 2017-25766